IEEE Access
Multidisciplinary : Rapid Review : Open Access Journal

Received March 18, 2022, accepted April 2, 2022, date of publication April 7, 2022, date of current version April 15, 2022.

Digital Object Identifier 10.1109/ACCESS.2022.3165567

Adaptive Neural Control of Uncertain MIMO Nonlinear Pure-Feedback Systems via Quantized State Feedback

BYUNG MO KIM AND SUNG JIN YOO, (Member, IEEE)
School of Electrical and Electronics Engineering, Chung-Ang University, Dongjak-Gu, Seoul 06974, South Korea
Corresponding author: Sung Jin Yoo (sjyoo@cau.ac.kr)

This work was supported by the National Research Foundation of Korea (NRF) grant funded by the Korea Government under Grant NRF-2019R1A2C1004898.

ABSTRACT We present an adaptive quantized state feedback tracking methodology for a class of uncertain multiple-input multiple-output (MIMO) nonlinear block-triangular pure-feedback systems with state quantizers. Uniform quantizers are considered to quantize all measurable state variables for feedback. Compared with the existing tracking approaches of MIMO lower-triangular nonlinear systems, the main contributions of the proposed strategy are developing (1) a quantized-state-feedback-based adaptive tracker in the presence of nonaffine interaction of states and control variables of MIMO systems and (2) an analysis strategy for quantized feedback stability using adaptive compensation terms to derive bounded quantization errors. In addition, the stability of the closed-loop system with quantized state feedback is analyzed based on the Lyapunov stability theorem. Finally, simulation examples, including interconnected inverted pendulums, are presented to validate the effectiveness of the proposed control strategy.

INDEX TERMS Quantized state feedback control, neural networks, state quantization, MIMO nonlinear systems, pure-feedback form.

I. INTRODUCTION

In the field of nonlinear control, adaptive recursive control techniques based on backstepping [1], dynamic surface design [2], and command-filtered backstepping design [3], [4] have been regarded as powerful tools for dealing with unmatched and uncertain nonlinearities. Adaptive control and filter designs using neural-network function approximators have been actively studied for systems with unknown nonlinearities (see [5]–[8] and references therein). To deal with more complex nonlinear systems, these techniques have been extended to multiple-input multiple-output (MIMO) nonlinear systems that include nonlinearities with couplings among system states and inputs. In [9], an adaptive fuzzy output feedback controller was designed for MIMO strict-feedback systems with unknown dead-zone inputs. In [10], an adaptive fuzzy tracking approach for MIMO nonlinear switched strict-feedback systems was studied. Adaptive neural control problems of MIMO pure-feedback nonlinear systems were addressed in [11] and [12]. In [13] and [14], fuzzy adaptive control approaches were developed for uncertain nonlinear multivariable systems. Moreover, the problems of output constraints [15] and event-triggered control [16] have been addressed for adaptive neural control designs of MIMO nonlinear systems. Contrary to these control designs using continuous feedback, industrial control systems based on digital networks require the transmission of quantized signals with finite values owing to band-limited communication channels [17]. Linear systems [18]–[20] and nonlinear control systems [21], [22] have been considered for quantized control. Several adaptive recursive control strategies have been investigated for uncertain lower-triangular single-input single-output nonlinear systems with quantized input signals [23]–[28]. Furthermore, these quantized control approaches have been adopted to address several control problems of input-quantized MIMO nonlinear systems. In [29], a tracking control problem using an observer was investigated for MIMO time-delay nonlinear systems in pure-feedback form. In [30], a prescribed performance control was proposed for interconnected MIMO nonlinear systems.

The associate editor coordinating the review of this manuscript and approving it for publication was Jinquan Xu.

An adaptive neural control problem of switched MIMO nonlinear systems with quantized dead-zone input was addressed in [31]. In [32], an adaptive input-quantized control approach was proposed for MIMO nonlinear systems with underactuated faults and time-varying output constraints. However, these successful quantized control approaches [23]–[32] are only feasible in the presence of input quantization. In network-based control systems, the quantization of measured state variables must be considered for feedback control design because the controller and MIMO systems are connected by band-limited network channels. To the best of our knowledge, quantized state feedback control design of uncertain MIMO pure-feedback nonlinear systems has not been investigated yet.

On the other hand, quantized-state-feedback-based recursive control design problems in the presence of state quantizers have been recently addressed for nonlinear systems with parametric uncertainties [33], [34]. Neural-network-based quantized feedback control designs were developed for strict-feedback nonlinear systems with time delays [35]. Furthermore, a distributed control strategy was presented for multi-agent nonlinear systems in strict-feedback form [36]. However, these approaches fail to provide a quantized state feedback control solution for MIMO nonlinear systems with coupling of state and control variables in pure-feedback form.

A primary difficulty in addressing this problem is to deal with unknown control coefficient matrices resulting from unknown nonaffine nonlinearities via quantized feedback information of states of all subsystems coupled in non-affine nonlinear form. Owing to unknown control coefficient matrices induced from unknown nonaffine nonlinearities, the quantized-state-based neural network adaptive control strategies reported in [35], [36] cannot be applied to ensure boundedness of close-loop quantization errors for the stability analysis of the closed-loop system. Therefore, it is important to establish quantized-state-based adaptive compensation strategies for tuning neural network approximators to guarantee that close-loop quantization errors are bounded in the presence of unknown control coefficient matrices.

To address this difficulty, we propose an adaptive quantized state feedback control methodology for uncertain MIMO nonlinear pure-feedback systems with state quantizers and external disturbances. All measurable state variables for feedback are quantized via state quantizers. An adaptive tracking scheme using quantized states is constructed in the presence of nonaffine nonlinear vectors and unknown bounds of gain matrices derived using the mean value theorem. In the proposed scheme, adaptive neural compensation terms using quantized state feedback are introduced to analyze quantization errors between unquantized and quantized signals in a closed-loop system. In addition, we analyze the boundedness of estimated parameters and quantization errors by establishing technical lemmas. Finally, the stability of the proposed control system is proved using the Lyapunov stability theorem. The main contributions of this study are as follows:

(i) Contrary to previous results [23]–[32] in which the input quantization problems were only considered in quantized control for MIMO lower-triangular nonlinear systems, this study addresses the state quantization problem for uncertain MIMO nonlinear pure-feedback systems. A neural-network-based quantized state feedback control strategy is developed to ensure the boundedness of quantization errors in the presence of unknown pure-feedback nonlinearities. In addition, adaptive function approximation terms and adaptive tuning laws using quantized states are constructed to compensate for unknown nonaffine nonlinearities and quantization errors.

(ii) In contrast to previous recursive tracker designs using quantized state feedback [33]–[36], this paper firstly deals with nonaffine nonlinearities interacting state variables and inputs in uncertain MIMO nonlinear systems. Moreover, a design difficulty caused by unknown gain matrices derived from the mean value theorem is resolved by introducing new adaptive approximation terms using quantized state feedback, contrary to [33]–[36]. The closed-loop stability based on quantized state feedback is investigated by analyzing the quantization errors.

The rest of the paper is organized as follows. The neural-network-based quantized state feedback tracking problem of MIMO nonlinear pure-feedback systems with state quantizers is described in Section II. The proposed adaptive quantized control design and stability analysis are discussed in Section III. Section IV presents simulation results including a practical example. Finally, we draw our conclusions in Section V.

II. PROBLEM FORMULATION

Consider the following uncertain MIMO block-triangular pure-feedback nonlinear system with external disturbances:

$$\begin{aligned}\dot{\boldsymbol{x}}_i &= \boldsymbol{f}_i(\bar{\boldsymbol{x}}_i, \boldsymbol{x}_{i+1}) + \boldsymbol{d}_i(t), \quad i = 1, \ldots, n-1 \\ \dot{\boldsymbol{x}}_n &= \boldsymbol{f}_n(\bar{\boldsymbol{x}}_n, \boldsymbol{u}) + \boldsymbol{d}_n(t) \\ \boldsymbol{y} &= \boldsymbol{x}_1 \end{aligned} \tag{1}$$

where $\boldsymbol{x}_i = [x_{i,1}, \ldots, x_{i,m}]^\top \in \mathbb{R}^m$ and $\bar{\boldsymbol{x}}_i = [\boldsymbol{x}_1^\top, \ldots, \boldsymbol{x}_i^\top]^\top \in \mathbb{R}^{im}$, $i = 1, \ldots, n$, are the state vectors, $\boldsymbol{y} = [y_1, \ldots, y_m]^\top \in \mathbb{R}^m$ is the system output vector, $\boldsymbol{u} = [u_1, \ldots, u_m]^\top \in \mathbb{R}^m$ is the control input vector, $\boldsymbol{f}_i(\bar{\boldsymbol{x}}_i, \boldsymbol{x}_{i+1}) = [f_{i,1}(\bar{\boldsymbol{x}}_i, x_{i+1,1}), \ldots, f_{i,m}(\bar{\boldsymbol{x}}_i, x_{i+1,m})]^\top \in \mathbb{R}^m$, $i = 1, \ldots, n-1$, and $\boldsymbol{f}_n(\bar{\boldsymbol{x}}_n, \boldsymbol{u}) = [f_{n,1}(\bar{\boldsymbol{x}}_n, u_1), \ldots, f_{n,m}(\bar{\boldsymbol{x}}_n, u_m)]^\top \in \mathbb{R}^m$ are the unknown C^1 nonaffine nonlinear function vectors, and $\boldsymbol{d}_i(t) \in \mathbb{R}^m$, $i = 1, \ldots, n$, is the external time-varying disturbance vector.

By applying the mean value theorem to the nonaffine functions $f_{i,j}(\bar{\boldsymbol{x}}_i, x_{i+1,j})$ and $f_{n,j}(\bar{\boldsymbol{x}}_n, u_j)$, $j = 1, \ldots, m$, we obtain [11]

$$\begin{aligned} f_{i,j}(\bar{\boldsymbol{x}}_i, x_{i+1,j}) &= f_{i,j}(\bar{\boldsymbol{x}}_i, 0) \\ &\quad + \left.\frac{\partial f_{i,j}}{\partial x_{i+1,j}}\right|_{x_{i+1,j}=\kappa_{i,j}} (x_{i+1,j} - 0) \\ f_{n,j}(\bar{\boldsymbol{x}}_n, u_j) &= f_{n,j}(\bar{\boldsymbol{x}}_n, 0) \end{aligned} \tag{2}$$

$$+ \frac{\partial f_{n,j}}{\partial u_j}\bigg|_{u_j=\kappa_{n,j}} (u_j - 0) \quad (3)$$

where $\kappa_{i,j} \in (0, x_{i+1,j})$ and $\kappa_{n,j} \in (0, u_j)$.

Then, $\boldsymbol{f}_i(\bar{\boldsymbol{x}}_i, \boldsymbol{x}_{i+1})$ and $\boldsymbol{f}_n(\bar{\boldsymbol{x}}_n, \boldsymbol{u})$ can be rewritten as

$$\boldsymbol{f}_i(\bar{\boldsymbol{x}}_i, \boldsymbol{x}_{i+1}) = \boldsymbol{f}_i(\bar{\boldsymbol{x}}_i) + \boldsymbol{G}_i\boldsymbol{x}_{i+1}, \quad i = 1, \ldots, n-1 \quad (4)$$

$$\boldsymbol{f}_n(\bar{\boldsymbol{x}}_n, \boldsymbol{u}) = \boldsymbol{f}_n(\bar{\boldsymbol{x}}_n) + \boldsymbol{G}_n\boldsymbol{u} \quad (5)$$

where $\boldsymbol{f}_i(\bar{\boldsymbol{x}}_i) = [f_{i,1}(\bar{\boldsymbol{x}}_i, 0), \ldots, f_{i,m}(\bar{\boldsymbol{x}}_i, 0)]^\top$, $\boldsymbol{f}_n(\bar{\boldsymbol{x}}_n) = [f_{n,1}(\bar{\boldsymbol{x}}_n, 0), \ldots, f_{n,m}(\bar{\boldsymbol{x}}_n, 0)]^\top$, $\boldsymbol{G}_i(\bar{\boldsymbol{x}}_i, \boldsymbol{\kappa}_i) = \partial \boldsymbol{f}_i(\bar{\boldsymbol{x}}_i, \boldsymbol{x}_{i+1}) / \partial \boldsymbol{x}_{i+1}|_{\boldsymbol{x}_{i+1}=\boldsymbol{\kappa}_i}$ with $\boldsymbol{\kappa}_i = [\kappa_{i,1}, \ldots, \kappa_{i,m}]^\top$, and $\boldsymbol{G}_n(\bar{\boldsymbol{x}}_n, \boldsymbol{\kappa}_n) = \partial \boldsymbol{f}_n(\bar{\boldsymbol{x}}_n, \boldsymbol{u})/\partial \boldsymbol{u}|_{\boldsymbol{u}=\boldsymbol{\kappa}_n}$ with $\boldsymbol{\kappa}_n = [\kappa_{n,1}, \ldots, \kappa_{n,m}]^\top$. Here, $\boldsymbol{G}_i$ and $\boldsymbol{G}_n$ are unknown gain matrices.

Using (4) and (5), the uncertain MIMO nonlinear system (1) becomes

$$\begin{aligned} \dot{\boldsymbol{x}}_i &= \boldsymbol{f}_i(\bar{\boldsymbol{x}}_i) + \boldsymbol{G}_i\boldsymbol{x}_{i+1} + \boldsymbol{d}_i(t), \quad i = 1, \ldots, n-1 \\ \dot{\boldsymbol{x}}_n &= \boldsymbol{f}_n(\bar{\boldsymbol{x}}_n) + \boldsymbol{G}_n\boldsymbol{u} + \boldsymbol{d}_n(t) \\ \boldsymbol{y} &= \boldsymbol{x}_1. \end{aligned} \quad (6)$$

Assumption 1: [37] The matrix $\boldsymbol{G}_i(\cdot)$, $i = 1, \ldots, n$ satisfies $0 < g_{i_m} \leq |\lambda(\boldsymbol{G}_i)| \leq g_{i_M}$ where $g_{i_m} > 0$ and $g_{i_M} > 0$ are unknown constants and $\lambda(\cdot)$ is the eigenvalue operator.

In this study, a network-based control problem using quantized state feedback is considered for system (1). In the network-based control problem, the system (1) and the controller are assumed to be connected through a network with a limited bandwidth. Thus, the measured state feedback information is transmitted to the controller after state quantization. For state quantization, the uniform quantizer is selected as follows:

$$Q(x_{i,j}) = \begin{cases} Z_\mu, & Z_\mu - \frac{\rho}{2} \leq x_{i,j} < Z_\mu + \frac{\rho}{2} \\ 0, & -\frac{\rho}{2} \leq x_{i,j} < \frac{\rho}{2} \\ -Z_\mu, & -Z_\mu - \frac{\rho}{2} \leq x_{i,j} < -Z_\mu + \frac{\rho}{2} \end{cases} \quad (7)$$

where $i = 1, \ldots, n$ and $j = 1, \ldots, m$, $\mu \in \mathbb{Z}^+$, ρ is the quantization level, $Z_1 = \rho$, and $Z_{\mu+1} = Z_\mu + \rho$. We use the definition $x_{i,j}^q \triangleq Q(x_{i,j})$ for notation simplicity. Then, using the property of the uniform quantizer, the state quantization error $\mu_{x_{i,j}} \triangleq x_{i,j} - x_{i,j}^q$ and its vector $\boldsymbol{\mu}_{x,i} \triangleq \boldsymbol{x}_i - \boldsymbol{x}_i^q$ satisfy $|\mu_{x_{i,j}}| \leq \rho$ and $\|\boldsymbol{\mu}_{x,i}\| \leq \rho\sqrt{m}$, respectively [18] where $\boldsymbol{x}_i^q = [x_{i,1}^q, \ldots, x_{i,m}^q]^\top$.

Remark 1: Owing to the uniformity of the quantization levels and simple structure, uniform quantizers facilitate the analysis of the quantization effect. Therefore, they are frequently utilized in analog-to-digital signal conversion [18]. For this reason, we use uniform quantizers (7) to quantize all measurable states for feedback. However, hysteresis-uniform or logarithmic-uniform quantizers can be also applied to the proposed approach.

Assumption 2 [33]: The quantized state vector $\boldsymbol{x}_i^q = [x_{i,1}^q, \ldots, x_{i,m}^q]^\top \in \mathbb{R}^m$, $i = 1, \ldots, n$, is available for feedback, rather than the unquantized state vector $\boldsymbol{x}_i$.

Assumption 3 [2]: The desired signal vector $\boldsymbol{x}_d \in \mathbb{R}^m$ and its time derivatives $\dot{\boldsymbol{x}}_d$ and $\ddot{\boldsymbol{x}}_d$ are bounded.

Assumption 4: The time-varying external disturbance vector $\boldsymbol{d}_i$, $i = 1, \ldots, n$, satisfies $\|\boldsymbol{d}_i\| \leq \bar{d}_i$ with an unknown constant $\bar{d}_i > 0$.

Lemma 1 [39]: For a Hurwitz matrix $\boldsymbol{A} \in \mathbb{R}^{m\times m}$ and a symmetric positive definite matrix $\boldsymbol{S} \in \mathbb{R}^{m\times m}$, the inequality $\|e^{\boldsymbol{A}t}\| \leq a_1 e^{-b_1 t}$ is ensured where $a_1 = \sqrt{\lambda_{\max}(\boldsymbol{S})/\lambda_{\min}(\boldsymbol{S})}$, $b_1 = 1/\lambda_{\max}(\boldsymbol{S})$, and $\lambda_{\max}(\boldsymbol{S})$ and $\lambda_{\min}(\boldsymbol{S})$ are the maximum and minimum eigenvalues of $\boldsymbol{S}$, respectively.

Problem 1: The control objective is to design a neural-network-based adaptive quantized state feedback control law $\boldsymbol{u}$ for uncertain MIMO pure-feedback nonlinear systems (1) with state quantizers (7) so that the output vector $\boldsymbol{y}(t)$ tracks the desired trajectory $\boldsymbol{x}_d(t)$, while all the closed-loop signals are bounded.

Remark 2: The validity of Assumptions 1–4 is explained as follows.

(i) The matrix $\boldsymbol{G}_i(\cdot)$ plays the role of the coefficient matrix for the virtual and actual control laws in the control design steps. $\boldsymbol{G}_i(\cdot) \neq 0$ should be assumed for controllability, which leads to $0 < g_{i_m} \leq |\lambda(\boldsymbol{G}_i)| \leq g_{i_M}$ in Assumption 1. This implies that $\boldsymbol{G}_i(\cdot)$ is strictly either positive or negative definite. Without loss of generality, it is assumed that $\boldsymbol{G}_i(\cdot) > 0$. Thus, Assumption 1 is reasonable.

(ii) Assumption 2 means that the state quantization problem is considered in this study. Thus, quantized state variables are available for feedback control design. This assumption is given for the problem formulation.

(iii) Assumption 3 implies that the desired signal and its first two derivatives are bounded. This assumption is reasonable for the recursive tracking control design objective.

(iv) Assumption 4 indicates that external disturbances may not grow arbitrarily large. This is common in existing control results.

Remark 3: For Problem 1, it is necessary to design a control law and adaptive tuning laws using quantized states in the presence of unknown nonaffine nonlinearities in MIMO form while ensuring the boundedness of quantization errors between the original and quantized signals. Furthermore, although quantized signals are used as inputs for neural network approximators, the boundedness of quantization errors and the closed-loop stability of the proposed neural-network-based control system should be proved. However, the existing adaptive control designs [23]–[32] dealing with input quantization of MIMO nonlinear systems use continuous state feedback information without state quantization. Thus, owing to the presence of quantized state feedback signals, Problem 1 cannot be addressed by the solutions proposed in [23]–[32].

III. NEURAL-NETWORK-BASED ADAPTIVE QUANTIZED STATE FEEDBACK CONTROL

A. RADIAL BASIS FUNCTION NEURAL NETWORKS

Unknown continuous nonlinear function vectors $\boldsymbol{N}_i(\boldsymbol{v}_i) \in \mathbb{R}^m$, $i = 1, \ldots, n$, can be approximated via radial basis function neural networks (RBFNNs) [40] in the compact set

$\Psi_i \subset \mathbb{R}^{p_i}$ as follows:

$$\boldsymbol{N}_i(\boldsymbol{\nu}_i) = \boldsymbol{\theta}_i^\top \boldsymbol{B}_i(\boldsymbol{\nu}_i) + \boldsymbol{\phi}_i(\boldsymbol{\nu}_i), \tag{8}$$

where $\boldsymbol{\nu}_i \in \Psi_i$ is the input vector of the RBFNN, $\boldsymbol{\theta}_i = \text{diag}[\boldsymbol{\theta}_{i,1}, \ldots, \boldsymbol{\theta}_{i,m}] \in \mathbb{R}^{mM_i \times m}$ is the ideal weighting matrix, $\boldsymbol{\theta}_{i,j} = [\theta_{i,j,1}, \ldots, \theta_{i,j,M_i}]^\top \in \mathbb{R}^{M_i}$, $j = 1, \ldots, m$, M_i is the number of neural nodes, $\boldsymbol{\phi}_i \in \mathbb{R}^m$, $i = 1, \ldots, n$ represents an approximation reconstruction error such that $\|\boldsymbol{\phi}_i\| \le \bar{\phi}_i$ with an unknown constant $\bar{\phi}_i > 0$, $\boldsymbol{B}_i = [\boldsymbol{B}_{i,1}^\top, \ldots, \boldsymbol{B}_{i,m}^\top]^\top \in \mathbb{R}^{mM_i}$; $\boldsymbol{B}_{i,j}(\iota) \in \mathbb{R}^{M_i}$, $j = 1, \ldots, m$, denotes the Gaussian function vector. Using the inherent property of Gaussian basis functions, it is ensured that $\|\boldsymbol{B}_i\| \le \bar{B}_i$ with a constant $\bar{B}_i > 0$ [41], [42].

Assumption 5: [41] $\boldsymbol{\theta}_i$ and $\boldsymbol{\phi}_i$ are bounded as $\|\boldsymbol{\theta}_i\| \le \bar{\theta}_i$ and $\|\boldsymbol{\phi}_i\| \le \bar{\phi}_i$, respectively, where $\bar{\theta}_i > 0$ and $\bar{\phi}_i > 0$ are constants.

B. ADAPTIVE CONTROL DESIGN USING QUANTIZED STATE FEEDBACK

The quantized state variables cannot be utilized directly in a Lyapunov-based systematic design because they are discontinuous. Thus, our design strategy is based on (i) designing the intermediate control signals using the unquantized state variables in **Step 1**, (ii) expressing the actual adaptive control input vector $\boldsymbol{u}$ using quantized state feedback in **Step 2**, and (iii) analyzing the quantization errors between unquantized and quantized signals to ensure the stability of the closed-loop system in the stability analysis part (see Section III-C).

Step 1: For the systematic control design of intermediate control signals, the command-filtered backstepping technique using second-order low-pass filters is employed. The error surfaces are expressed as follows:

$$\begin{aligned} z_1 &= \boldsymbol{x}_1 - \boldsymbol{x}_d \\ z_{i+1} &= \boldsymbol{x}_{i+1} - \boldsymbol{\alpha}_{i,f} \\ \tilde{\boldsymbol{\alpha}}_i &= \boldsymbol{\alpha}_{i,f} - \boldsymbol{\alpha}_i \end{aligned} \tag{9}$$

where $i = 1, \ldots, n-1$, $z_1 = [z_{1,1}, \ldots, z_{1,m}]^\top \in \mathbb{R}^m$ and $z_{i+1} = [z_{i+1,1}, \ldots, z_{i+1,m}]^\top \in \mathbb{R}^m$ are error surfaces, $\boldsymbol{\alpha}_i = [\alpha_{1,1}, \ldots, \alpha_{1,m}]^\top \in \mathbb{R}^m$ are intermediate control laws, and $\boldsymbol{\alpha}_{i,f} = [\alpha_{1f,1}, \ldots, \alpha_{1f,m}]^\top \in \mathbb{R}^m$ are their corresponding filtered signals provided by the following second-order low-pass filters:

$$\begin{aligned} \dot{\boldsymbol{\alpha}}_{i,f} &= \boldsymbol{\beta}_i \\ \dot{\boldsymbol{\beta}}_i &= -2\boldsymbol{\xi}_i \boldsymbol{\varpi}_i \boldsymbol{\beta}_i - \boldsymbol{\varpi}_i^\top \boldsymbol{\varpi}_i (\boldsymbol{\alpha}_{i,f} - \boldsymbol{\alpha}_i) \end{aligned} \tag{10}$$

with $\boldsymbol{\alpha}_{i,f}(0) = \boldsymbol{\alpha}_i(0)$, $\boldsymbol{\beta}_i(0) = 0$, and the filter constant matrices $\boldsymbol{\xi}_i = \text{diag}[\xi_{i,1}, \ldots, \xi_{i,m}]$ and $\boldsymbol{\varpi}_i = \text{diag}[\varpi_{i,1}, \ldots, \varpi_{i,m}]$. Here, $\xi_{i,j} > 0$ and $\varpi_{i,j} > 0$, $j = 1, \ldots, m$, denote the damping ratio and natural frequency, respectively. The intermediate control laws $\boldsymbol{\alpha}_i$ are established as follows.

(i) The time derivative of z_1 along (6) is given by

$$\dot{z}_1 = \boldsymbol{f}_1 + \boldsymbol{G}_1 \boldsymbol{x}_2 + \boldsymbol{d}_1 - \dot{\boldsymbol{x}}_d. \tag{11}$$

Let us consider the Lyapunov function V_1 as follows:

$$V_1 = \frac{1}{2g_{1_M}} z_1^\top z_1. \tag{12}$$

Differentiating V_1 with respect to time yields

$$\dot{V}_1 \le z_1^\top \left(\boldsymbol{N}_1 + \frac{\boldsymbol{G}_1}{g_{1_M}} \boldsymbol{x}_2 + \frac{\boldsymbol{d}_1}{g_{1_M}} \right) \tag{13}$$

where $\boldsymbol{N}_1(\boldsymbol{\nu}_1) = (\boldsymbol{f}_1 - \dot{\boldsymbol{x}}_d)/g_{1_M}$; $\boldsymbol{\nu}_1 = [\boldsymbol{x}_1^\top, \dot{\boldsymbol{x}}_d^\top]^\top$. Using (8), the unknown function $\boldsymbol{N}_1$ is approximated by $\boldsymbol{N}_1(\boldsymbol{\nu}_1) = \boldsymbol{\theta}_1^\top \boldsymbol{B}_1(\boldsymbol{\nu}_1) + \boldsymbol{\phi}_1(\boldsymbol{\nu}_1)$. Then, (13) becomes

$$\dot{V}_1 \le z_1^\top \left(\boldsymbol{\theta}_1^\top \boldsymbol{B}_1 + \boldsymbol{\phi}_1 + \frac{\boldsymbol{G}_1}{g_{1_M}} \boldsymbol{x}_2 + \frac{\boldsymbol{d}_1}{g_{1_M}} \right). \tag{14}$$

From Assumptions 1 and 5, it holds that

$$\begin{aligned} z_1^\top \boldsymbol{\theta}_1^\top \boldsymbol{B}_1 &\le \frac{g_{1_m}}{g_{1_M}} z_1^\top z_1 + \frac{g_{1_M}}{4g_{1_m}} \|\boldsymbol{B}_1\|^2 \|\boldsymbol{\theta}_1\|^2 \\ &\le \frac{1}{g_{1_M}} z_1^\top \boldsymbol{G}_1 z_1 + \frac{g_{1_m}}{g_{1_M}} \|\boldsymbol{B}_1\|^2 W_1 \end{aligned} \tag{15}$$

where $W_1 = (g_{1_M}^2 / 4g_{1_m}^2)\bar{\theta}_1^2$. Then, (13) becomes

$$\begin{aligned} \dot{V}_1 \le{}& \frac{1}{g_{1_M}} z_1^\top \boldsymbol{G}_1 (z_1 + z_2 + \tilde{\boldsymbol{\alpha}}_1 + \boldsymbol{\alpha}_1) \\ &+ z_1^\top \left(\boldsymbol{\phi}_1 + \frac{\boldsymbol{d}_1}{g_{1_M}} \right) + \frac{g_{1_m}}{g_{1_M}} \|\boldsymbol{B}_1\|^2 W_1. \end{aligned} \tag{16}$$

The intermediate signal $\boldsymbol{\alpha}_1$ is designed as follows

$$\boldsymbol{\alpha}_1 = -(\zeta_1 + 1) z_1 - \frac{z_1 \|\boldsymbol{B}_1\|^2 \hat{W}_1}{(z_1^\top z_1 + \bar{\varepsilon})} - \hat{\delta}_1 \tanh\left(\frac{z_1}{\boldsymbol{\epsilon}_1} \right) \tag{17}$$

where ζ_1 is a design parameter, $\tanh(z_1/\boldsymbol{\epsilon}_1) = [\tanh(z_{1,1}/\epsilon_{1,1}), \ldots, \tanh(z_{1,m}/\epsilon_{1,m})]^\top \in \mathbb{R}^m$; $\epsilon_{1,j} > 0, j = 1, \ldots, m$, are design parameters, $\bar{\varepsilon}$ is a design parameter satisfying $\bar{\varepsilon} \ge 1/4$, and $\hat{W}_1$ is the estimate of W_1, and $\hat{\delta}_1$ is the estimate of an unknown constant $\delta_1 > 0$, which is defined subsequently.

Substituting (17) into (16) gives

$$\begin{aligned} \dot{V}_1 \le{}& -\frac{1}{g_{1_M}} \zeta_1 z_1^\top \boldsymbol{G}_1 z_1 + \frac{1}{g_{1_M}} z_1^\top \boldsymbol{G}_1 (z_2 + \tilde{\boldsymbol{\alpha}}_1) \\ &- \frac{z_1^\top \boldsymbol{G}_1 z_1}{g_{1_M}(z_1^\top z_1 + \bar{\varepsilon})} \|\boldsymbol{B}_1\|^2 (W_1 + \tilde{W}_1) \\ &+ \frac{g_{1_m}}{g_{1_M}} \|\boldsymbol{B}_1\|^2 W_1 + z_1^\top \left(\boldsymbol{\phi}_1 + \frac{\boldsymbol{d}_1}{g_{1_M}} \right) \\ &- \frac{1}{g_{1_M}} z_1^\top \boldsymbol{G}_1 (\tilde{\delta}_1 + \delta_1) \tanh\left(\frac{z_1}{\boldsymbol{\epsilon}_1} \right) \end{aligned} \tag{18}$$

where $\tilde{\delta}_1 = \hat{\delta}_1 - \delta_1$ and $\tilde{W}_1 = \hat{W}_1 - W_1$ are the estimation errors.

Then, using $-z_1^\top \boldsymbol{G}_1 z_1 \le -g_{1_m} z_1^\top z_1$, we have

$$\begin{aligned} &-\frac{z_1^\top \boldsymbol{G}_1 z_1}{g_{1_M}(z_1^\top z_1 + \bar{\varepsilon})} \|\boldsymbol{B}_1\|^2 W_1 + \frac{g_{1_m}}{g_{1_M}} \|\boldsymbol{B}_1\|^2 W_1 \\ &= \frac{-z_1^\top \boldsymbol{G}_1 z_1 \|\boldsymbol{B}_1\|^2 W_1 + g_{1_m} z_1^\top z_1 \|\boldsymbol{B}_1\|^2 W_1}{g_{1_M}(z_1^\top z_1 + \bar{\varepsilon})} \end{aligned}$$

$$+\frac{g_{1_m}\bar{\varepsilon}\|\boldsymbol{B}_1\|^2W_1}{g_{1_M}(z_1^\top z_1+\bar{\varepsilon})}$$
$$\leq\frac{g_{1_m}\bar{\varepsilon}\|\boldsymbol{B}_1\|^2W_1}{g_{1_M}(z_1^\top z_1+\bar{\varepsilon})}. \tag{19}$$

Thus, (18) becomes

$$\begin{aligned}\dot{V}_1\leq&-\frac{1}{g_{1_M}}\zeta_1 z_1^\top \boldsymbol{G}_1 z_1+\frac{1}{g_{1_M}}z_1^\top \boldsymbol{G}_1(z_2+\tilde{\boldsymbol{\alpha}}_1)\\&+\frac{g_{1_m}\bar{\varepsilon}\|\boldsymbol{B}_1\|^2W_1}{g_{1_M}(z_1^\top z_1+\bar{\varepsilon})}-\frac{z_1^\top \boldsymbol{G}_1 z_1}{g_{1_M}(z_1^\top z_1+\bar{\varepsilon})}\|\boldsymbol{B}_1\|^2\tilde{W}_1\\&+z_1^\top\left(\boldsymbol{\phi}_1+\frac{\boldsymbol{d}_1}{g_{1_M}}\right)-\frac{1}{g_{1_M}}z_1^\top \boldsymbol{G}_1\delta_1\tanh\left(\frac{z_1}{\boldsymbol{\epsilon}_1}\right)\\&-\frac{1}{g_{1_M}}z_1^\top \boldsymbol{G}_1\tilde{\delta}_1\tanh\left(\frac{z_1}{\boldsymbol{\epsilon}_1}\right).\end{aligned} \tag{20}$$

(ii) The time derivative of z_i along (6) is given by

$$\dot{z}_i=\boldsymbol{f}_i+\boldsymbol{G}_i\boldsymbol{x}_{i+1}-\dot{\boldsymbol{\alpha}}_{i-1,f}+\boldsymbol{d}_i \tag{21}$$

where $i=2,\ldots,n-1$.

Consider the Lyapunov function $V_i=(1/(2g_{i_M}))z_i^\top z_i$. Differentiating V_i with respect to time yields

$$\dot{V}_i=\frac{1}{g_{i_M}}z_i^\top(\boldsymbol{f}_i+\boldsymbol{G}_i\boldsymbol{x}_{i+1}-\boldsymbol{\beta}_{i-1}+\boldsymbol{d}_i) \tag{22}$$

where $\dot{\boldsymbol{\alpha}}_{i-1,f}=\boldsymbol{\beta}_{i-1}$ is used from (10).

Adding and subtracting $z_{i-1}^\top \boldsymbol{G}_{i-1}z_i/g_{(i-1)_M}$, (22) becomes

$$\dot{V}_i=z_i^\top\left(\boldsymbol{N}_i+\frac{\boldsymbol{G}_i}{g_{i_M}}\boldsymbol{x}_{i+1}+\frac{\boldsymbol{d}_i}{g_{i_M}}\right)-\frac{1}{g_{(i-1)_M}}z_{i-1}^\top \boldsymbol{G}_{i-1,i}z_i \tag{23}$$

where $\boldsymbol{N}_i(\boldsymbol{\nu}_i)=(\boldsymbol{f}_i-\boldsymbol{\beta}_{i-1})/g_{i_M}+\boldsymbol{G}_{i-1}^\top z_{i-1}/g_{(i-1)_M}$; $\boldsymbol{\nu}_i=[\bar{\boldsymbol{x}}_i^\top, z_{i-1}^\top, \boldsymbol{\beta}_{i-1}^\top]^\top$. From (8), the unknown function $\boldsymbol{N}_i$ is approximated as $\boldsymbol{N}_i(\boldsymbol{\nu}_i)=\boldsymbol{\theta}_i^\top\boldsymbol{B}_i(\boldsymbol{\nu}_i)+\boldsymbol{\phi}_i(\boldsymbol{\nu}_i)$. Similar to (15), it holds that

$$z_i^\top\boldsymbol{\theta}_i^\top\boldsymbol{B}_i\leq\frac{1}{g_{i_M}}z_i^\top\boldsymbol{G}_i z_i+\frac{g_{i_m}}{g_{i_M}}\|\boldsymbol{B}_i\|^2W_i \tag{24}$$

where $W_i=(g_{i_M}^2/4g_{i_m}^2)\bar{\theta}_i^2$. Using (24), (23) becomes

$$\dot{V}_i=\frac{1}{g_{i_M}}z_i^\top\boldsymbol{G}_i(z_i+z_{i+1}+\tilde{\boldsymbol{\alpha}}_i+\boldsymbol{\alpha}_i)+z_i^\top\left(\boldsymbol{\phi}_i+\frac{\boldsymbol{d}_i}{g_{i_M}}\right)-\frac{1}{g_{(i-1)_M}}z_{i-1}^\top\boldsymbol{G}_{i-1}z_i+\frac{g_{i_m}}{g_{i_M}}\|\boldsymbol{B}_i\|^2W_i. \tag{25}$$

Let us design the intermediate signal $\boldsymbol{\alpha}_i$ as

$$\boldsymbol{\alpha}_i=-(\zeta_i+1)z_i-\frac{z_i\|\boldsymbol{B}_i\|^2\hat{W}_i}{(z_i^\top z_i+\bar{\varepsilon})}-\hat{\delta}_i\tanh\left(\frac{z_i}{\boldsymbol{\epsilon}_i}\right) \tag{26}$$

where ζ_i is a design parameter, $\tanh(z_i/\boldsymbol{\epsilon}_i)=[\tanh(z_{i,1}/\epsilon_{i,1}),\ldots,\tanh(z_{i,m}/\epsilon_{i,m})]^\top\in\mathbb{R}^m$; $\epsilon_{i,j}>0$, $j=1,\ldots,m$, are design parameters, and $\hat{W}_i$ and $\hat{\delta}_i$ are estimates of W_i and an unknown constant $\delta_i>0$ to be defined later, respectively.

Substituting (26) into (25) and using the inequality as in (19) yields

$$\begin{aligned}\dot{V}_i\leq&-\frac{1}{g_{i_M}}\zeta_i z_i^\top\boldsymbol{G}_i z_i+\frac{1}{g_{i_M}}z_i^\top\boldsymbol{G}_i(z_{i+1}+\tilde{\boldsymbol{\alpha}}_i)\\&-\frac{1}{g_{(i-1)_M}}z_{i-1}^\top\boldsymbol{G}_{i-1,i}z_i+\frac{g_{i_m}\bar{\varepsilon}\|\boldsymbol{B}_i\|^2W_i}{g_{i_M}(z_i^\top z_i+\bar{\varepsilon})}\\&-\frac{z_i^\top\boldsymbol{G}_i z_i}{g_{i_M}(z_i^\top z_i+\bar{\varepsilon})}\|\boldsymbol{B}_i\|^2\tilde{W}_i+z_i^\top\left(\boldsymbol{\phi}_i+\frac{\boldsymbol{d}_i}{g_{i_M}}\right)\\&-\frac{1}{g_{i_M}}z_i^\top\boldsymbol{G}_i(\delta_i+\tilde{\delta}_i)\tanh\left(\frac{z_i}{\boldsymbol{\epsilon}_i}\right)\end{aligned} \tag{27}$$

where $\tilde{\delta}_i=\hat{\delta}_i-\delta_i$ and $\tilde{W}_i=\hat{W}_i-W_i$ are the estimation errors.

(iii) The time derivative of z_n along (6) is given by

$$\dot{z}_n=\boldsymbol{f}_n+\boldsymbol{G}_n\boldsymbol{u}-\dot{\boldsymbol{\alpha}}_{n-1,f}+\boldsymbol{d}_n. \tag{28}$$

Consider the Lyapunov function $V_n=(1/(2g_{n_M}))z_n^\top z_n$. Differentiating V_n with respect to time yields

$$\dot{V}_n=\frac{1}{g_{n_M}}z_n^\top(\boldsymbol{f}_n+\boldsymbol{G}_n\boldsymbol{u}-\boldsymbol{\beta}_{n-1}+\boldsymbol{d}_n). \tag{29}$$

Adding and subtracting $z_{n-1}^\top\boldsymbol{G}_{n-1}z_n/g_{(n-1)_M}$, (29) becomes

$$\dot{V}_n=z_n^\top\left(\boldsymbol{N}_n+\frac{\boldsymbol{G}_n}{g_{n_M}}\boldsymbol{u}+\frac{\boldsymbol{d}_n}{g_{n_M}}\right)-\frac{1}{g_{(n-1)_M}}z_{n-1}^\top\boldsymbol{G}_{n-1}z_n \tag{30}$$

where $\boldsymbol{N}_n(\boldsymbol{\nu}_n)=(\boldsymbol{f}_n-\boldsymbol{\beta}_{n-1})/g_{n_M}+\boldsymbol{G}_{n-1}^\top z_{n-1}/g_{(n-1)_M}$; $\boldsymbol{\nu}_n=[\bar{\boldsymbol{x}}_n^\top, z_{n-1}^\top, \boldsymbol{\beta}_{n-1}^\top]^\top$. Using (8), the unknown function $\boldsymbol{N}_n$ is approximated as $\boldsymbol{N}_n(\boldsymbol{\nu}_n)=\boldsymbol{\theta}_n^\top\boldsymbol{B}_n(\boldsymbol{\nu}_n)+\boldsymbol{\phi}_n(\boldsymbol{\nu}_n)$. Then, similar to (15), it holds that

$$z_n^\top\boldsymbol{\theta}_n^\top\boldsymbol{B}_n\leq\frac{1}{g_{n_M}}z_n^\top\boldsymbol{G}_n z_n+\frac{g_{n_m}}{g_{n_M}}\|\boldsymbol{B}_n\|^2W_n \tag{31}$$

where $W_n=(g_{n_M}^2/4g_{n_m}^2)\bar{\theta}_n^2$. Using (31), (30) becomes

$$\dot{V}_n=\frac{1}{g_{n_M}}z_n^\top\boldsymbol{G}_n(\boldsymbol{\mu}_u+z_n+\boldsymbol{v})+z_n^\top\left(\boldsymbol{\phi}_n+\frac{\boldsymbol{d}_n}{g_{n_M}}\right)-\frac{1}{g_{(n-1)_M}}z_{n-1}^\top\boldsymbol{G}_{n-1}z_n+\frac{g_{n_m}}{g_{n_M}}\|\boldsymbol{B}_n\|^2W_n \tag{32}$$

where $\boldsymbol{\mu}_u=\boldsymbol{u}-\boldsymbol{v}$ and $\boldsymbol{v}$ is an intermediate signal.

Let us design the intermediate signal $\boldsymbol{v}$ as

$$\boldsymbol{v}=-(\zeta_n+1)z_n-\frac{z_n\|\boldsymbol{B}_n\|^2\hat{W}_n}{(z_n^\top z_n+\bar{\varepsilon})}-\hat{\delta}_n\tanh\left(\frac{z_n}{\boldsymbol{\epsilon}_n}\right) \tag{33}$$

where ζ_n is a design parameter, $\tanh(z_n/\boldsymbol{\epsilon}_n)=[\tanh(z_{n,1}/\epsilon_{n,1}),\ldots,\tanh(z_{n,m}/\epsilon_{n,m})]^\top\in\mathbb{R}^m$; $\epsilon_{n,j}>0$, $j=1,\ldots,m$, are design parameters, $\hat{W}_n$, and $\hat{\delta}_n$ are estimates of W_n and an unknown constant $\delta_n>0$ to be defined later, repectively.

Substituting (33) into (32) and using the following inequality

$$-\frac{z_n^\top\boldsymbol{G}_n z_n}{g_{n_M}(z_n^\top z_n+\bar{\varepsilon})}\|\boldsymbol{B}_n\|^2W_n+\frac{g_{n_m}}{g_{n_M}}\|\boldsymbol{B}_n\|^2W_n\leq\frac{g_{n_m}\bar{\varepsilon}\|\boldsymbol{B}_n\|^2W_n}{g_{n_M}(z_n^\top z_n+\bar{\varepsilon})}. \tag{34}$$

gives

$$\dot{V}_n = \frac{1}{g_{nM}} z_n^\top G_n \mu_u - \frac{1}{g_{nM}} \zeta_n z_n^\top G_n z_n - \frac{1}{g_{(n-1)M}} z_{n-1}^\top G_{n-1} z_n + \frac{g_{n_m} \bar{\varepsilon} \|B_n\|^2 W_n}{g_{nM}(z_n^\top z_n + \bar{\varepsilon})} - \frac{z_n^\top G_n z_n}{g_{nM}(z_n^\top z_n + \bar{\varepsilon})} \|B_n\|^2 \tilde{W}_n + z_n^\top \left(\phi_n + \frac{d_n}{g_{nM}} \right) - \frac{1}{g_{nM}} z_n^\top G_n (\delta_n + \tilde{\delta}_n) \tanh\left(\frac{z_n}{\epsilon_n} \right) \quad (35)$$

where $\tilde{\delta}_n = \hat{\delta}_n - \delta_n$ and $\tilde{W}_n = \hat{W}_n - W_n$ are the estimation errors.

Step 2: In this step, we present a quantized-state-based control law u based on the structures of the error surfaces and the intermediate signals designed in Step 1. Owing to the recursive design property of a quantized-state-based control law u, all error surfaces and intermediate signals designed in Step 1 are redefined using quantized states.

The error surfaces using state quantization are defined as

$$z_1^* = x_1^q - x_d$$
$$z_{i+1}^* = x_{i+1}^q - \alpha_{i,f}^* \quad (36)$$

where $i = 1, \ldots, n-1$, and $\alpha_{i,f}^*$ are the command-filtered signals of the virtual control laws α_i^* using quantized states expressed as

$$\dot{\alpha}_{i,f}^* = \beta_i^*$$
$$\dot{\beta}_i^* = -2\xi_i \varpi_i \beta_i^* - \varpi_i^\top \varpi_i (\alpha_{i,f}^* - \alpha_i^*) \quad (37)$$

with $\alpha_{i,f}^*(0) = \alpha_i^*(0)$ and $\beta_i^*(0) = 0$.

Then, we introduce the quantized-state-feedback-based virtual control laws α_i^* and the adaptive actual control law u as follows:

$$\alpha_i^* = -(\zeta_i + 1) z_i^* - \frac{z_i^*}{((z_i^*)^\top z_i^* + \bar{\varepsilon})} \|B_i^*\|^2 \hat{W}_i - \hat{\delta}_i \tanh\left(\frac{z_i^*}{\epsilon_i} \right) \quad (38)$$

$$u = -(\zeta_n + 1) z_n^* - \frac{z_n^*}{((z_n^*)^\top z_n^* + \bar{\varepsilon})} \|B_n^*\|^2 \hat{W}_n - \hat{\delta}_n \tanh\left(\frac{z_n^*}{\epsilon_n} \right) \quad (39)$$

$$\dot{\hat{W}}_j = \Gamma_{W,j} (\|z_j^*\|^2 \|B_j^*\|^2 - \sigma_{W,j} \|z_j^*\|^2 \hat{W}_j) \quad (40)$$

$$\dot{\hat{\delta}}_j = \Gamma_{\delta,j} \left((z_j^*)^\top \tanh\left(\frac{z_j^*}{\epsilon_j} \right) - \sigma_{\delta,j} \|z_j^*\| \hat{\delta}_j \right) \quad (41)$$

where $i = 1, \ldots, n-1$, $j = 1, \ldots, n$, $B_j^* = B_j(v_j^*)$; $v_1^* = [(x_1^q)^\top, \dot{x}_d^\top]^\top$, $v_k^* = [(\bar{x}_k^q)^\top, (z_{k-1}^*)^\top, (\beta_{k-1}^*)^\top]^\top$, $k = 2, \ldots, n$, $\Gamma_{W,j} > 0$ and $\Gamma_{\delta,j} > 0$ are tuning gains, and $\sigma_{W,j}$ and $\sigma_{\delta,j}$ are positive constants for σ-modification. A block diagram of the proposed state feedback adaptive tracking system is shown in Fig. 1.

Remark 4: Compared with previous recursive tracking results using quantized state feedback [33]–[36], we introduce the neural-network-based adaptive compensation terms $-\frac{z_i^*}{((z_i^*)^\top z_i^* + \bar{\varepsilon})} \|B_i^*\|^2 \hat{W}_i$, $i = 1, \ldots, n$, in (38) and (39). Thus, we enable the analysis of the boundedness of the quantization errors in the presence of unknown control coefficient matrices G_i, which will be presented in the next section. The stability of the quantized state feedback adaptive tracking system is analyzed based on these terms. Furthermore, the adaptive laws (40) and (41) using quantized states are derived to ensure that the estimates $\hat{W}_j$ and $\hat{\delta}_j$ are bounded, as proved in the next section.

Remark 5: Using the second-order command filter (37), $\dot{\alpha}_{i,f}^*$, $i = 1, \ldots, n-1$, are replaced by the continuous signals β_i^* in the control laws (38) and (39) where β_i^* are included in the inputs of neural networks. Thus, from the recursive design procedure, we attenuate the unexpected chattering effects caused by $\dot{\alpha}_{i,f}^*$ in the control law u.

C. STABILITY ANALYSIS

Define $\bar{\tilde{\alpha}}_j = [\tilde{\alpha}_1^\top, \ldots, \tilde{\alpha}_j^\top]^\top$, $\bar{\beta}_j = [\beta_1^\top, \ldots, \beta_j^\top]^\top$, $\bar{z}_i = [z_1^\top, \ldots, z_i^\top]^\top$, $\bar{\hat{W}}_i = [\hat{W}_1, \ldots, \hat{W}_i]^\top$, $\bar{\hat{\delta}}_i = [\hat{\delta}_1, \ldots, \hat{\delta}_i]^\top$, $\bar{x}_d = [x_d^\top, \dot{x}_d^\top, \ddot{x}_d^\top]^\top$, and $\bar{d}_i = [d_1^\top, \ldots, d_i^\top]^\top$ for $j = 1, \ldots, n-1$ and $i = 1, \ldots, n$. Then, the time derivative $\chi_j = [\tilde{\alpha}_j^\top, \beta_j^\top]^\top$ along (10) is obtained as

$$\dot{\chi}_j = \Lambda_j \chi_j + H P_j \quad (42)$$

where $\Lambda_j = \begin{bmatrix} 0 & I \\ -\varpi_j^\top \varpi_j & -2\xi_j \varpi_j \end{bmatrix}$, $H = \begin{bmatrix} I \\ 0 \end{bmatrix}$; $0 \in R^{m \times m}$ denotes the matrix with zero elements, $I \in R^{m \times m}$ is the identity matrix, and

$$P_1(\bar{z}_2, \tilde{\alpha}_1, \hat{W}_1, \hat{\delta}_1, \bar{x}_d, d_1) = (\zeta_1 + 1)\dot{z}_1 + \frac{\dot{z}_1 (z_1^\top z_1 + \bar{\epsilon}) - 2 z_1 z_1^\top \dot{z}_1}{(z_1^\top z_1 + \bar{\epsilon})^2} \|B_1\|^2 \hat{W}_1 + \frac{2 z_1}{(z_1^\top z_1 + \bar{\epsilon})} B_1^\top \dot{B}_1 \hat{W}_1 + \frac{z_1}{(z_1^\top z_1 + \bar{\epsilon})} \|B_1\|^2 \dot{\hat{W}}_1 + \dot{\hat{\delta}}_1 \tanh\left(\frac{z_1}{\epsilon_1} \right) + \hat{\delta}_1 \mathrm{sech}^2\left(\frac{z_1}{\epsilon_1} \right) \frac{\dot{z}_1}{\epsilon_1}$$

$$P_k(\bar{z}_{k+1}, \bar{\tilde{\alpha}}_k, \bar{\beta}_{k-1}, \bar{\hat{W}}_k, \bar{\hat{\delta}}_k, \bar{x}_d, \bar{d}_k) = (\zeta_k + 1)\dot{z}_k + \frac{\dot{z}_k (z_k^\top z_k + \bar{\epsilon}) - 2 z_k z_k^\top \dot{z}_k}{(z_k^\top z_k + \bar{\epsilon})^2} \|B_k\|^2 \hat{W}_k + \frac{2 z_k}{(z_k^\top z_k + \bar{\epsilon})} B_k^\top \dot{B}_k \hat{W}_k + \frac{z_k}{(z_k^\top z_k + \bar{\epsilon})} \|B_k\|^2 \dot{\hat{W}}_k + \dot{\hat{\delta}}_k \tanh\left(\frac{z_k}{\epsilon_k} \right) + \hat{\delta}_k \mathrm{sech}^2\left(\frac{z_k}{\epsilon_k} \right) \frac{\dot{z}_k}{\epsilon_k}$$

for $k = 2, \ldots, n-1$. Here, Λ_j are Hurwitz matrices due to $\xi_{j,l} > 0$ and $\varpi_{j,l} > 0$, $l = 1, \ldots, m$. Thus, for any matrix $Q_j > 0$, $\Lambda_j^\top S_j + S_j \Lambda_j = -Q_j$ is ensured with a symmetric matrix $S_j > 0$.

Lemma 2: For the adaptive laws (40) and (41), there exist compact sets $\Psi_{W,i} = \{\tilde{W}_i | |\tilde{W}_i| \leq \Omega_{W,i}\}$ with a constant $\Omega_{W,i}$ and $\Psi_{\delta,i} = \{\tilde{\delta}_i | |\tilde{\delta}_i| \leq \Omega_{\delta,i}\}$ with a constant $\Omega_{\delta,i}$ such that $\tilde{W}_i(t) \in \Psi_{W,i}$ and $\tilde{\delta}_i(t) \in \Psi_{\delta,i}$, $\forall t \geq 0$ provided that $\tilde{W}_i(0) \in \Psi_{W,i}$ and $\tilde{\delta}_i(0) \in \Psi_{\delta,i}$, respectively, where $i = 1, \ldots, n$.

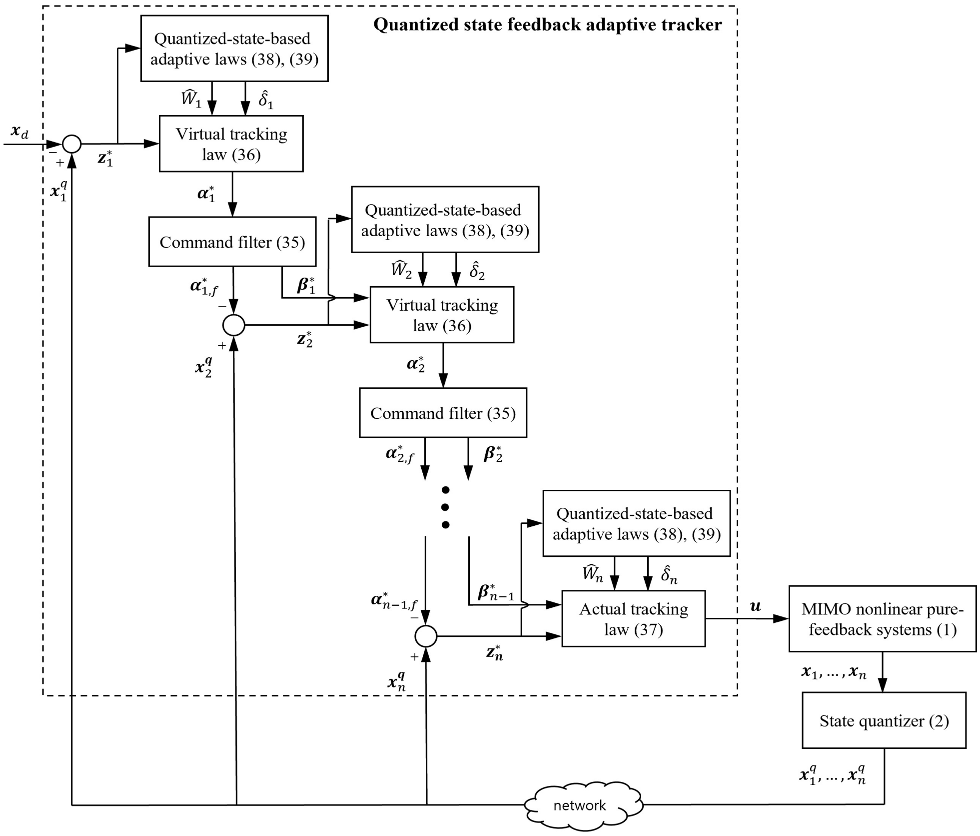

FIGURE 1. Block diagram of the proposed quantized state feedback adaptive tracking system.

Proof: To prove the boundedness of $\tilde{W}_i$, consider a Lyapunov function candidate $V_{W,i} = (1/2\Gamma_{W,i})\tilde{W}_i^2$. Then, from $\|\boldsymbol{\theta}_i\| \le \bar{\theta}_i$, $\|\boldsymbol{B}_i\| \le \bar{B}_i$, and $\|\boldsymbol{B}_i^*\| \le \bar{B}_i$, the time derivative of $V_{W,i}$ is obtained as

$$\begin{aligned}\dot{V}_{W,i} &= \|z_i^*\|^2\tilde{W}_i(\|\boldsymbol{B}_i^*\|^2 - \sigma_{W,i}\hat{W}_i)\\ &\le \|z_i^*\|^2|\tilde{W}_i|(\bar{B}_i^2 + \sigma_{W,i}w_i\bar{\theta}_i^2 - \sigma_{W,i}|\tilde{W}_i|). \quad (43)\end{aligned}$$

where $w_i = (g_{i_M}^2/4g_{i_m}^2)$. Therefore, it is ensured that $\dot{V}_{W,i} < 0$ when $|\tilde{W}_i| > \Omega_{W,i}$ with $\Omega_{W,i} \triangleq (\bar{B}_i^2 + \sigma_{W,i}w_i\bar{\theta}_i^2)/\sigma_{W,i}$. Thus, $V_{W,i}$ decreases when $W_i(t) \notin \Psi_{W,i}$, and $W_i(t)$ remains within $\Psi_{W,i}$.

Let us show the boundedness of $\tilde{\delta}_i$ by considering $V_{\delta,i} = (1/2\Gamma_{\delta,i})\tilde{\delta}_i^2$. From $\|\tanh(z_i^*/\boldsymbol{\epsilon}_i)\| \le \sqrt{m}$ and $\hat{\delta}_i = \delta_i + \tilde{\delta}_i$, it holds that

$$\dot{V}_{\delta,i} \le |\tilde{\delta}_i|\|z_i^*\|(\sqrt{m} + \sigma_{\delta,i}\delta_i - \sigma_{\delta,i}|\tilde{\delta}_i|). \quad (44)$$

Therefore, it is ensured that $\dot{V}_{\delta,i} < 0$ when $|\tilde{\delta}_i| > \Omega_{\delta,i}$ with $\Omega_{\delta,i} \triangleq (\sqrt{m} + \sigma_{\delta,i}\delta_i)/\sigma_{\delta,i}$. Thus, $V_{\delta,i}$ decreases when $\delta_i(t) \notin \Psi_{\delta,i}$, and $\delta_i(t)$ remains within $\Psi_{\delta,i}$. If $\delta_i(0) \in \Psi_{\delta,i}$, $\delta_i(t) \in \Psi_{\delta,i}$ for all $t \ge 0$. This completes the proof of this lemma. ■

Lemma 3: Define the quantization error vectors of the closed-loop signals as

$$\begin{aligned}\boldsymbol{\mu}_{z,i} &= z_i - z_i^*, \quad \boldsymbol{\mu}_{\alpha,j} = \boldsymbol{\alpha}_j - \boldsymbol{\alpha}_j^*\\ \boldsymbol{\mu}_{\alpha,j,f} &= \boldsymbol{\alpha}_{j,f} - \boldsymbol{\alpha}_{j,f}^*, \quad \boldsymbol{\mu}_{\beta,j} = \boldsymbol{\beta}_j - \boldsymbol{\beta}_j^*\end{aligned}$$

where $i = 1, \ldots, n$ and $j = 1, \ldots, n-1$, and consider the quantization errors of the control input $\boldsymbol{\mu}_u = \boldsymbol{u} - \boldsymbol{v}$. Then, there exist positive constants $\Delta_{z,i}$, $\Delta_{\alpha,j}$, $\Delta_{\chi,j}$, and Δ_u such that $\|\boldsymbol{\mu}_{z,i}\| \le \Delta_{z,i}$, $\|\boldsymbol{\mu}_{\alpha,j}\| \le \Delta_{\alpha,j}$, $\|\boldsymbol{\mu}_{\chi,j}\| \le \Delta_{\chi,j}$, and $\|\boldsymbol{\mu}_u\| \le \Delta_u$, respectively, where $\boldsymbol{\mu}_{\chi,j} = [\boldsymbol{\mu}_{\alpha,j,f}^\top, \boldsymbol{\mu}_{\beta,j}^\top]^\top$.

Proof: We prove this lemma following a recursive approach.

(i) From the property $\|\boldsymbol{\mu}_{x,i}\| \le \rho\sqrt{m}$ and $\boldsymbol{\mu}_{z,1} = z_1 - z_1^*$, it holds that

$$\|\boldsymbol{\mu}_{z,1}\| = \|\boldsymbol{\mu}_{x,1}\| \le \rho\sqrt{m} \triangleq \Delta_{z,1}. \quad (45)$$

Lemma 2 leads to $|\tilde{W}_1| \le \bar{\Omega}_{W,1}$ and $|\tilde{\delta}_1| \le \bar{\Omega}_{\delta,1}$ where $\bar{\Omega}_{W,1} = \max\{|\tilde{W}_1(0)|, \Omega_{W,1}\}$ and $\bar{\Omega}_{\delta,1} = \max\{|\tilde{\delta}_1(0)|, \Omega_{\delta,1}\}$. From the boundedness of W_1 and δ_1, there exist unknown constants $\bar{\hat{W}}_1$ and $\bar{\hat{\delta}}_1$ that satisfy $|\hat{W}_1| \le \bar{\hat{W}}_1$ and $|\hat{\delta}_1| \le \bar{\hat{\delta}}_1$. Using (17) and (38), we obtain

$$\begin{aligned}\boldsymbol{\mu}_{\alpha,1} = &-(\zeta_1 + 1)(z_1 - z_1^*) - \left(\frac{z_1}{(z_1^\top z_1 + \bar{\varepsilon})}\|\boldsymbol{B}_1\|^2\right.\\ &\left. - \frac{z_1^*}{((z_1^*)^\top z_1^* + \bar{\varepsilon})}\|\boldsymbol{B}_1^*\|^2\right)\hat{W}_1\\ &- \hat{\delta}_1\left(\tanh\left(\frac{z_1}{\boldsymbol{\epsilon}_1}\right) - \tanh\left(\frac{z_1^*}{\boldsymbol{\epsilon}_1}\right)\right). \quad (46)\end{aligned}$$

Here, $\|z_1/(z_1^\top z_1 + \bar{\varepsilon})\| \le 1$ is satisfied because of $\bar{\varepsilon} \ge 1/4$. Using the inequalities $\|\boldsymbol{B}_i - \boldsymbol{B}_i^*\| \le 2\bar{B}_i$ and

$\|\tanh(\frac{z_i}{\epsilon_i}) - \tanh(\frac{z_i^*}{\epsilon_i})\| \le 2\sqrt{m}$, $i = 1, \ldots, n$, we have

$$\|\mu_{\alpha,1}\| \le (\zeta_1 + 1)\Delta_{z,1} + 2\bar{B}_1\bar{\hat{W}}_1 + 2\bar{\hat{\delta}}_1\sqrt{m} \triangleq \Delta_{\alpha,1}. \tag{47}$$

From (10) and (37), the time derivative of the quantization error $\mu_{\chi,1} = [\mu_{\alpha,1,f}, \mu_{\beta,1}]^\top$ is given by

$$\dot{\mu}_{\chi,1} = \Lambda_1\mu_{\chi,1} + H_1\mu_{\alpha,1} \tag{48}$$

where $\Lambda_1 = \begin{bmatrix} 0 & I \\ -\varpi_1^\top\varpi_1 & -2\xi_1\varpi_1 \end{bmatrix}$ and $H_1 = [0, \varpi_1^\top\varpi_1]^\top$. Thus, the solution of (48) is obtained as

$$\mu_{\chi,1}(t) = e^{\Lambda_1 t}\mu_{\chi,1}(0) + \int_0^t e^{\Lambda_1(t-\tau)}H_1\mu_{\alpha,1}(\tau)d\tau. \tag{49}$$

From $\|\mu_{\alpha,1}\| \le \Delta_{\alpha,1}$, we have that for all $t \ge 0$,

$$\|\mu_{\chi,1}(t)\| \le \|e^{\Lambda_1 t}\|\|\mu_{\chi,1}(0)\| + \Delta_{\alpha,1}\|H_1\|\|\Lambda_1^{-1}(I - e^{\Lambda_1 t})\|. \tag{50}$$

From Lemma 1, the inequality $\|e^{\Lambda_1 t}\| \le a_1 e^{-b_1 t}$ is ensured where $a_1 > 0$ and $b_1 > 0$ are constants. Thus, (50) is expressed as

$$\|\mu_{\chi,1}(t)\| \le a_1\|\mu_{\chi,1}(0)\| + \Delta_{\alpha,1}\|H_1\|\|\Lambda_1^{-1}\|(1 + a_1) \triangleq \Delta_{\chi,1}. \tag{51}$$

It is satisfied that $\|\mu_{\alpha,1,f}\| \le \Delta_{\chi,1}$ and $\|\mu_{\beta,1}\| \le \Delta_{\chi,1}$.

(ii) Owing to $\|\mu_{x,j}\| \le \rho\sqrt{m}$, $\mu_{z,j}$ is bounded as

$$\|\mu_{z,j}\| \le \|\mu_{x,j}\| + \|\mu_{\alpha,j-1,f}\| \le \rho\sqrt{m} + \Delta_{\chi,j-1} \triangleq \Delta_{z,j} \tag{52}$$

where $j = 2, \ldots, n-1$. Using (26), (38), and the inequality $\|z_j/(z_j^\top z_j + \bar{\varepsilon})\| \le 1$, $\mu_{\alpha,j}$ is bounded as

$$\|\mu_{\alpha,j}\| \le \Delta_{\alpha,j} \tag{53}$$

where $\Delta_{\alpha,j} \triangleq (\zeta_j + 1)\Delta_{z,j} + 2\bar{B}_j\bar{\hat{W}}_j + 2\bar{\hat{\delta}}_j\sqrt{m}$ with positive unknown constants $\bar{\hat{W}}_j$ and $\bar{\hat{\delta}}_j$ satisfying $|\hat{W}_j| \le \bar{\hat{W}}_j$ and $|\hat{\delta}_j| \le \bar{\hat{\delta}}_j$, respectively. Similar to (48)-(51), there exists a constant $\Delta_{\chi,j}$ such that $\|\mu_{\alpha,j,f}\| \le \Delta_{\chi,j}$ and $\|\mu_{\beta,j}\| \le \Delta_{\chi,j}$.

(iii) Similar to (52), it is satisfied that

$$\|\mu_{z,n}\| \le \Delta_{z,n} \tag{54}$$

where $\Delta_{z,n} = \rho\sqrt{m} + \Delta_{\chi,n-1}$. Then, from (33) and (39), we obtain

$$\mu_u = -(\zeta_n + 1)(z_n - z_n^*) - \left(\frac{z_n}{(z_n^\top z_n + \bar{\varepsilon})}\|B_n\|^2 - \frac{z_n^*}{((z_n^*)^\top z_n^* + \bar{\varepsilon})}\|B_n^*\|^2\right)\hat{W}_n - \hat{\delta}_n\left(\tanh\left(\frac{z_n}{\epsilon_n}\right) - \tanh\left(\frac{z_n^*}{\epsilon_n}\right)\right). \tag{55}$$

Then, using $\|z_n/(z_n^\top z_n + \bar{\varepsilon})\| \le 1$, μ_u is bounded as

$$\|\mu_u\| \le \Delta_u \tag{56}$$

where $\Delta_u \triangleq (\zeta_n + 1)\Delta_{z,n} + 2\bar{B}_n\bar{\hat{W}}_n + 2\bar{\hat{\delta}}_n\sqrt{m}$ with positive unknown constants $\bar{\hat{W}}_n$ and $\bar{\hat{\delta}}_n$ satisfying $|\hat{W}_n| \le \bar{\hat{W}}_n$ and $|\hat{\delta}_n| \le \bar{\hat{\delta}}_n$, respectively. This completes the proof. ∎

Choose the overall Lyapunov function candidate V as

$$V = \sum_{i=1}^n V_i + \sum_{j=1}^{n-1}\chi_j^\top S_j\chi_j \tag{57}$$

where $S_j > 0$ is a symmetric matrix.

Remark 6: Contrary to the existing neural-network-based adaptive control approaches considering state quantization [34]–[36], this paper deals with the problem of unknown control coefficient function matrices G_i in the control design procedure. Specifically, the minimal parameter technique is employed to tune the unknown parameters W_i, $i = 1, \ldots, n$ including the norm of the weights of RBFNNs. The minimal parameter technique is commonly used in the form $z_i\|B_i\|^2\hat{W}_i$ in the existing studies for uncertain nonlinear pure-feedback systems [12], [15], [16], [28], [29]. However, this form cannot be directly adopted in our quantized state feedback controller because the boundedness of the quantization errors $z_i\|B_i\|^2\hat{W}_i - z_i^*\|B_i^*\|^2\hat{W}_i$ cannot be analyzed based on the boundedness of $\mu_{z,i}$ and B_i^* in Lemma 3. Thus, we introduce adaptive neural compensation terms $z_i\|B_i\|^2\hat{W}_i/(z_i^\top z_i + \bar{\varepsilon})$ in the proposed tracker (i.e., (38) and (39)) and the inequality $z_i\|B_i\|^2\hat{W}_i/(z_i^\top z_i + \bar{\varepsilon}) \le \bar{B}_i^2\hat{W}_i$ is employed in the proof of Lemma 3.

Theorem 1: Consider an uncertain MIMO pure-feedback nonlinear system (1) with state quantizers (7) where state variables and control inputs are fully interconnected in the block-triangular pure-feedback form. Then, for any initial conditions satisfying $V(0) \le \psi$ with a constant $\psi > 0$, the neural-network-based quantized adaptive tracking scheme consisting of (38)–(41) ensures uniform ultimate boundedness of all closed-loop signals using quantized feedback and the convergence of the tracking error z_1 to an arbitrarily small neighborhood of the origin.

Proof: Substituting (20), (27), (35), and (42) into the time derivative of V yields

$$\begin{aligned}\dot{V} \le & -\sum_{i=1}^n \frac{1}{g_{iM}}\zeta_i z_i^\top G_i z_i - \sum_{j=1}^{n-1}\chi_j^\top Q_j\chi_j \\ & + 2\sum_{j=1}^{n-1}\chi_j^\top S_j H P_j + \sum_{j=1}^{n-1}\frac{1}{g_{jM}}z_j^\top G_j\tilde{\alpha}_j \\ & + \sum_{i=1}^n \frac{g_{im}}{g_{iM}}z_i^\top\bar{\delta}_i - \sum_{i=1}^n \frac{1}{g_{iM}}z_i^\top G_i\delta_i\tanh\left(\frac{z_i}{\epsilon_i}\right) \\ & - \sum_{i=1}^n \frac{1}{g_{iM}}z_i^\top G_i\tilde{\delta}_i\tanh\left(\frac{z_i}{\epsilon_i}\right) \\ & + \sum_{i=1}^n \frac{g_{im}\bar{\varepsilon}\|B_i\|^2 W_i}{g_{iM}(z_i^\top z_i + \bar{\varepsilon})}\end{aligned} \tag{58}$$

where

$$\breve{\delta}_j = \frac{1}{g_{j_m}}\left(g_{j_M}\boldsymbol{\phi}_j + \boldsymbol{d}_j - \frac{\boldsymbol{G}_j z_j\|\boldsymbol{B}_j\|^2\tilde{W}_j}{(z_j^\top z_j + \bar{\varepsilon})}\right)$$
$$\breve{\delta}_n = \frac{1}{g_{n_m}}\left(g_{n_M}\boldsymbol{\phi}_n + \boldsymbol{d}_n - \frac{\boldsymbol{G}_n z_n\|\boldsymbol{B}_n\|^2\tilde{W}_n}{(z_n^\top z_n + \bar{\varepsilon})} + \boldsymbol{G}_n\boldsymbol{\mu}_u\right)$$

with $j = 1, \ldots, n-1$. From Assumptions 4 and 5, and Lemma 2, there exist positive unknown constants $\bar{\phi}_i$, $\bar{d}_i$, $\bar{B}_i$, and $\bar{\Omega}_{W,i}$ such that $\|\boldsymbol{\phi}_i\| \le \bar{\phi}_i$, $\|\boldsymbol{d}_i\| \le \bar{d}_i$, $\|\boldsymbol{B}_i\| \le \bar{B}_i$ and $|\tilde{W}_i| \le \bar{\Omega}_{W,i}$, $i = 1, \ldots, n$ and $z_i/(z_i^\top z_i + \bar{\varepsilon})$ satisfies $\|z_i/(z_i^\top z_i + \bar{\varepsilon})\| \le 1$ for any positive constants $\bar{\varepsilon} \ge 1/4$. Then, δ_i, $i = 1, \ldots, n$, are defined as

$$\|\breve{\boldsymbol{\delta}}_j\| \le \frac{1}{g_{j_m}}(g_{j_M}\bar{\phi}_j + \bar{d}_j + g_{j_M}\bar{B}_j^2\bar{\Omega}_{W,j}\sqrt{m}) \triangleq \delta_j \quad (59)$$
$$\|\breve{\boldsymbol{\delta}}_n\| \le \frac{1}{g_{n_m}}(g_{n_M}\bar{\phi}_n + \bar{d}_n + g_{n_M}\bar{B}_n^2\bar{\Omega}_{W,n}\sqrt{m} + g_{n_M}\Delta_u) \triangleq \delta_n \quad (60)$$

where $j = 1, \ldots, n-1$. From (59) and (60), we obtain the following inequality

$$\begin{aligned}\frac{g_{i_m}}{g_{i_M}}z_i^\top\breve{\boldsymbol{\delta}}_i - \frac{1}{g_{i_M}}z_i^\top\boldsymbol{G}_i\delta_i\tanh\left(\frac{z_i}{\boldsymbol{\epsilon}_i}\right) &\le \frac{g_{i_m}}{g_{i_M}}\delta_i\left(\|z_i\| - z_i^\top\tanh\left(\frac{z_i}{\boldsymbol{\epsilon}_i}\right)\right)\\ &\le \sum_{j=1}^{m}0.2785\epsilon_{i,j}\delta_i. \end{aligned} \quad (61)$$

Using (61), (58) becomes

$$\begin{aligned}\dot{V} \le &-\sum_{i=1}^{n}\frac{g_{i_m}}{g_{i_M}}\zeta_i z_i^\top z_i - \sum_{j=1}^{n-1}q_{j_m}\|\boldsymbol{\chi}_j\|^2\\ &+2\sum_{j=1}^{n-1}\boldsymbol{\chi}_j^\top\boldsymbol{S}_j\boldsymbol{H}\boldsymbol{P}_j + \sum_{j=1}^{n-1}\frac{1}{g_{j_M}}z_j^\top\boldsymbol{G}_j\tilde{\boldsymbol{\alpha}}_j\\ &-\sum_{i=1}^{n}\frac{1}{g_{i_M}}z_i^\top\boldsymbol{G}_i\tilde{\delta}_i\tanh\left(\frac{z_i}{\boldsymbol{\epsilon}_i}\right)\\ &+\sum_{i=1}^{n}\frac{g_{i_m}\bar{\varepsilon}\|\boldsymbol{B}_i\|^2W_i}{g_{i_M}(z_i^\top z_i + \bar{\varepsilon})} + \sum_{i=1}^{n}\sum_{j=1}^{m}0.2785\epsilon_{i,j}\delta_i \end{aligned} \quad (62)$$

where q_{j_m} is the minimum eigenvalue of $\boldsymbol{Q}_j$. Since $\boldsymbol{d}_j$, $\tilde{W}_j$, and $\tilde{\delta}_j$ are bounded, there exist positive functions $\breve{\boldsymbol{P}}_j$ such that

$$\begin{aligned}&\|\boldsymbol{P}_1(\bar{z}_2, \tilde{\boldsymbol{\alpha}}_1, \bar{\boldsymbol{x}}_d, \hat{W}_1, \hat{\delta}_1, \boldsymbol{d}_1)\| \le \breve{\boldsymbol{P}}_1(\bar{z}_2, \tilde{\boldsymbol{\alpha}}_1, \bar{\boldsymbol{x}}_d)\\ &\|\boldsymbol{P}_k(\bar{z}_{k+1}, \bar{\tilde{\boldsymbol{\alpha}}}_k, \bar{\boldsymbol{\beta}}_{k-1}, \bar{\boldsymbol{x}}_d, \bar{\hat{W}}_k, \bar{\hat{\delta}}_k, \bar{\boldsymbol{d}}_k)\|\\ &\quad \le \breve{\boldsymbol{P}}_k(\bar{z}_{k+1}, \bar{\tilde{\boldsymbol{\alpha}}}_k, \bar{\boldsymbol{\beta}}_{k-1}, \bar{\boldsymbol{x}}_d) \end{aligned} \quad (63)$$

where $k = 2, \ldots, n-1$. Let us define the compact sets $\digamma_j \in \mathbb{R}^{(3j+1)m}$, $j = 1, \ldots, n-1$, and $\digamma_d \in \mathbb{R}^{3m}$ as $\digamma_j = \{\sum_{l=1}^{j+1}z_l^\top z_l + 2\sum_{l=1}^{j}\boldsymbol{\chi}_l^\top\boldsymbol{S}_l\boldsymbol{\chi}_l \le 2\psi\}$, and $\digamma_d = \{\boldsymbol{x}_d^\top\boldsymbol{x}_d + \dot{\boldsymbol{x}}_d^\top\dot{\boldsymbol{x}}_d + \ddot{\boldsymbol{x}}_d^\top\ddot{\boldsymbol{x}}_d \le \varsigma_d\}$ with a constant $\varsigma_d > 0$. Then, there exists a constant $\bar{P}_j$ satisfying $\|\breve{\boldsymbol{P}}_j\| \le \bar{P}_j$ on a compact set $\digamma_j \times \digamma_d$. This yields

$$\begin{aligned}2\boldsymbol{\chi}_j^\top\boldsymbol{S}_j\boldsymbol{H}\boldsymbol{P}_j &\le \frac{\|\breve{\boldsymbol{P}}_j\|^2\|\boldsymbol{S}_j\|^2\|\boldsymbol{\chi}_j\|^2}{\breve{\epsilon}} + \breve{\epsilon}\\ \frac{1}{g_{j_M}}z_j^\top\boldsymbol{G}_j\tilde{\boldsymbol{\alpha}}_j &\le \frac{1}{2}\|z_j\|^2 + \frac{1}{2}\|\boldsymbol{\chi}_j\|^2\\ -\frac{\tilde{\delta}_i}{g_{i_M}}z_i^\top\boldsymbol{G}_i\tanh\left(\frac{z_i}{\boldsymbol{\epsilon}_i}\right) &\le \frac{1}{2}\|z_i\|^2 + \frac{m}{2}\bar{\Omega}_{\delta,i}^2\\ \frac{g_{i_m}\bar{\varepsilon}\|\boldsymbol{B}_i\|^2W_i}{g_{i_M}(z_i^\top z_i + \bar{\varepsilon})} &\le w_i\bar{B}_i^2\bar{\theta}_i^2 \end{aligned}$$

where $j = 1, \ldots, n-1$, $i = 1, \ldots, n$, and $\breve{\epsilon} > 0$ is a constant. By selecting design parameters as $\zeta_i = g_{i_M}(\bar{\zeta}_i + 1)/g_{i_m}$, $\zeta_n = g_{n_M}(\bar{\zeta}_n + 1/2)/g_{n_m}$, and $q_{i_m} = 1/2 + \bar{P}_i^2\|\boldsymbol{S}_i\|^2/\breve{\epsilon} + \bar{q}_{i_m}$, $i = 1, \ldots, n-1$, with positive constants $\bar{\zeta}_i$, $\bar{\zeta}_n$, and $\bar{q}_{i_m}$, (62) becomes

$$\begin{aligned}\dot{V} \le &-\sum_{i=1}^{n}\bar{\zeta}_i\|z_i\|^2 - \sum_{j=1}^{n-1}\bar{q}_{j_m}\|\boldsymbol{\chi}_j\|^2\\ &-\sum_{j=1}^{n-1}\left(1 - \frac{\|\breve{\boldsymbol{P}}_j\|^2}{\bar{P}_j^2}\right)\frac{\bar{P}_j^2\|\boldsymbol{S}_j\|^2\|\boldsymbol{\chi}_j\|^2}{\breve{\epsilon}} + C \end{aligned} \quad (64)$$

where $C = \sum_{i=1}^{n}(w_i\bar{B}_i^2\bar{\theta}_i^2 + m\bar{\Omega}_{\delta,i}^2/2 + \sum_{j=1}^{m}0.2785\epsilon_{i,j}\delta_i) + \breve{\epsilon}(n-1)$. Since $\|\breve{\boldsymbol{P}}_j\| \le \bar{P}_j$ on $V = \psi$, the inequality (64) becomes $\dot{V} \le -\zeta V + C$ where $\zeta = \min_{i=1,\ldots,n, j=1,\ldots,n-1}\{2\bar{\zeta}_i g_{i_M}, \bar{q}_{j_m}/\lambda_{max}(\boldsymbol{S}_j)\}$. When $\zeta > C/\psi$, $\dot{V} < 0$ on $V = \psi$, which leads to the invariant set $V \le \psi$. Then, it is shown that z_i and $\boldsymbol{\chi}_j$, $i = 1, \ldots, n$, $j = 1, \ldots, n-1$, are bounded. From the boundedness of z_1 and $\boldsymbol{x}_d$, $\boldsymbol{x}_1$ is bounded and $\boldsymbol{\alpha}_1$ in (17) is bounded according to the boundedness of $\hat{W}_1$ and $\hat{\delta}_1$ from Lemma 2. Moreover, the boundedness of $\boldsymbol{\alpha}_1$ results in the boundedness of $\boldsymbol{\alpha}_{1,f}$ and $\boldsymbol{\beta}_1$ with the stable filter (10). Then, $\boldsymbol{x}_2$ is bounded according to the boundedness of z_2 and $\boldsymbol{\alpha}_{1,f}$. Using a similar argument, $\boldsymbol{x}_i$, $\boldsymbol{\alpha}_j$, $\boldsymbol{\alpha}_{j,f}$, $\boldsymbol{\beta}_j$, and $\boldsymbol{v}$ are bounded for $i = 1, \ldots, n$, $j = 1, \ldots, n-1$. Thus, using Lemma 3, $\boldsymbol{\alpha}_j^*$, $\boldsymbol{\alpha}_{j,f}^*$ and $\boldsymbol{\beta}_j^*$ are also bounded and we conclude that the actual control input $\boldsymbol{u}$ is bounded. Furthermore, $(1/2g_{1_M})z_1^\top z_1 \le V(t) \le e^{-\zeta t}V(0) + (C/\zeta)(1 - e^{-\zeta t})$ is satisfied from $\dot{V} \le -\zeta V + C$. Thus, the tracking error z_1 is reduced to an adjustable compact set $\Upsilon = \{z_1 | \|z_1\| \le \sqrt{2g_{1_M}C/\zeta}\}$ by choosing design parameters. ■

Remark 7: The control performance can be improved by reducing the compact set Υ in the proof of Theorem 1. In this direction, the guidelines for the design parameters of the proposed adaptive quantized state feedback controller are as follows.

(i) Increasing the control gains ζ_i, $i = 1, \ldots, n$, helps in increasing ζ and consequently Υ can be reduced.

(ii) C in Υ can be reduced by reducing the quantization level ρ as long as the network resources allow, and by decreasing the design parameters $\epsilon_{i,j}$, $i = 1, \ldots, n$, $j = 1, \ldots, m$. Then, the compact set Υ can be reduced.

(iii) Selecting the filter constants $\boldsymbol{\varpi}_i$ and $\boldsymbol{\xi}_i$ appropriately helps in increasing the minimum eigenvalue q_{i_m} of $\boldsymbol{Q}_i$,

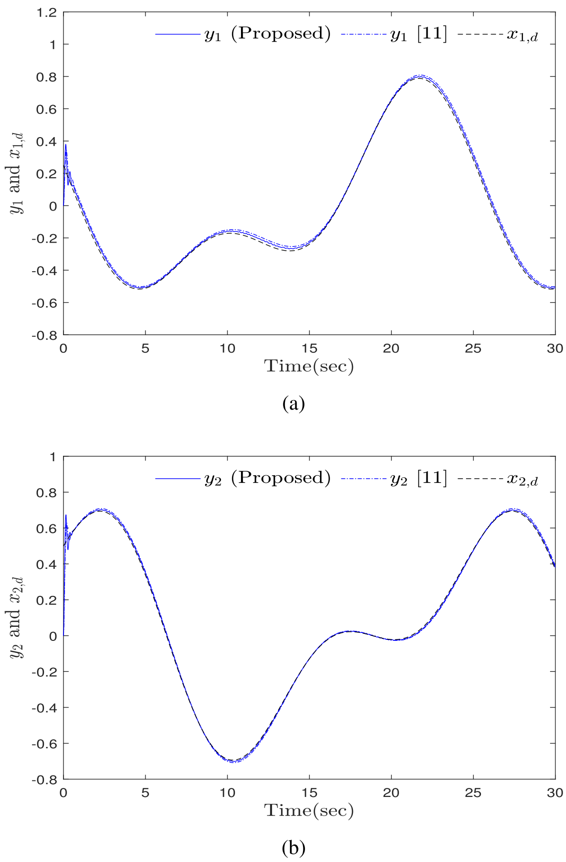

FIGURE 2. Tracking results for Example 1 (a) $x_{1,d}$ and y_1 (b) $x_{2,d}$ and y_2.

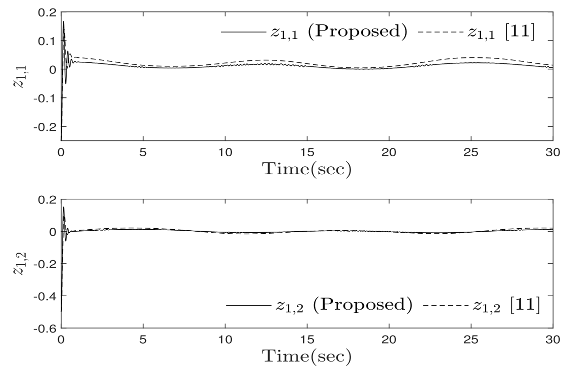

FIGURE 3. Control errors $z_{1,1}$ and $z_{1,2}$ for Example 1.

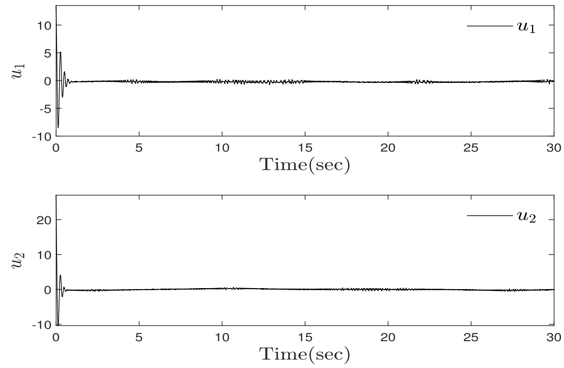

FIGURE 4. Control inputs u_1 and u_2 for Example 1.

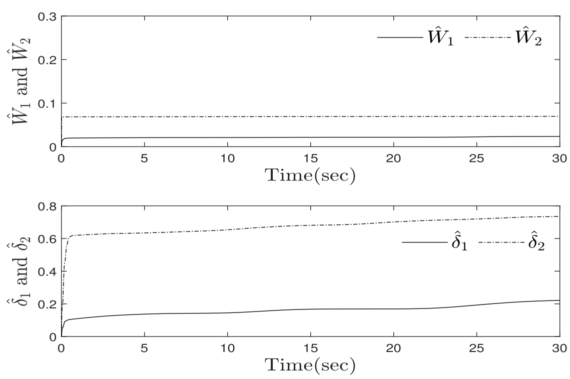

FIGURE 5. Estimates of W_1, W_2, δ_1 and δ_2 for Example 1.

$i = 1, \dots, n-1$, which subsequently increases ζ. Consequently, the compact set Υ is then reduced.

(iv) Increasing the tuning gains $\Gamma_{W,i}$ and $\Gamma_{\delta,i}$, $i = 1, \dots, n$ and fixing $\sigma_{W,i}$ and $\sigma_{\delta,j}$ as small values help to increase the learning speed of the estimated vectors $\hat{W}_i$ and parameters $\hat{\delta}_j$.

Remark 8: In [43], a fuzzy adaptive output feedback control approach was presented for MIMO nonlinear systems with full-states prescribed performance in finite-time. In [44], a finite-time adaptive quantized control problem was investigated for stochastic systems in presence of input quantization. The finite-time controllers designed in [43], [44] are based on non-quantized state variables (i.e., continuous state feedback information). To apply the proposed state-quantized design approach to the finite-time control problem, a finite-time control design ensuring bounded quantization errors, as reported in Lemma 3, should be newly developed. Therefore, it will be interesting to address the finite-time control problem based on quantized state feedback of MIMO nonlinear pure-feedback systems in future studies.

IV. SIMULATION RESULTS

To demonstrate the effectiveness of our theoretical tracking strategy in the presence of state quantization, we present two examples including interconnected inverted pendulums. In addition, we compare the tracking performance of the proposed state-quantized controller and the existing tracking controller [11] designed without state quantization.

Example 1: The following MIMO nonlinear system is considered:

$$\begin{aligned} \dot{\boldsymbol{x}}_1 &= \boldsymbol{f}_1(\boldsymbol{x}_1, \boldsymbol{x}_2) + \boldsymbol{d}_1 \\ \dot{\boldsymbol{x}}_2 &= \boldsymbol{f}_2(\bar{\boldsymbol{x}}_2, \boldsymbol{u}) + \boldsymbol{d}_2 \\ \boldsymbol{y}_1 &= \boldsymbol{x}_1 \end{aligned} \tag{65}$$

where $\boldsymbol{x}_1 = [x_{1,1}, x_{1,2}]^\top$, $\boldsymbol{x}_2 = [x_{2,1}, x_{2,2}]^\top$, and

$$\boldsymbol{f}_1(\boldsymbol{x}_1, \boldsymbol{x}_2) = \begin{bmatrix} (4 + \sin(x_{1,1}x_{1,2}))x_{2,1} + 0.3\cos(x_{2,1}) \\ (2 + \cos(x_{1,1}x_{1,2}))x_{2,2} + 0.7\sin(x_{2,2}) \end{bmatrix}$$

$$\boldsymbol{f}_2(\bar{\boldsymbol{x}}_2, \boldsymbol{u}) = \begin{bmatrix} x_{2,2}e^{-x_{1,1}x_{2,1}^2} + (2 + x_{1,2}^2)u_1 + 0.5\cos(u_1) \\ x_{1,2}e^{-x_{2,1}x_{1,2}^2} + (3 + x_{1,1}^2)u_2 + 0.3\sin(u_2) \end{bmatrix}$$

$$\boldsymbol{d}_1 = \begin{bmatrix} 0.15\cos(0.5t) \\ 0.15\sin(0.5t) \end{bmatrix}, \ \boldsymbol{d}_2 = \begin{bmatrix} 0.1\cos(t) \\ 0.1\sin(t) \end{bmatrix}.$$

Here, the unknown nonaffine nonlinearities $\boldsymbol{f}_1$ and $\boldsymbol{f}_2$ include the interactions of the state variables and control inputs. The desired signal vector is set to $\boldsymbol{x}_d = [-0.3\sin(0.5t) + 0.5\cos(0.25t + \pi/3), 0.3\sin(0.5t) + 0.5\cos(0.25t)]^\top$. The initial conditions of the state variables are set as $\boldsymbol{x}_1 = [0, 0]^\top$ and $\boldsymbol{x}_2 = [0, 0]^\top$. The quantization level is set to $\rho = 0.005$. The design parameters of the proposed state-quantized adaptive tracker are chosen to be $\zeta_1 = 5$, $\zeta_2 = 7$, $\Gamma_{W,i} = 3$, $\Gamma_{\delta,i} = 1.5$, $\sigma_{W,i} = 0.01$, $\sigma_{\delta,i} = 0.1$, $\epsilon_{i,1} = \epsilon_{i,2} = 0.08$, $\bar{\varepsilon} = 0.25$, $\xi_{1,1} = \xi_{1,2} = 0.707$, $\varpi_{1,1} = 80$, and $\varpi_{1,2} = 80$ where $i = 1, 2$. The control gains and weight tuning parameters of the existing adaptive tracker [11] are set to be identical to those of the proposed tracker.

The quantized state feedback tracking results and errors of the proposed state-quantized adaptive tracker and the previous adaptive tracker [11] are compared in Figs. 2 and 3. The time responses of the system outputs and desired signals are compared in Fig. 2 and those of the tracking errors are displayed in Fig. 3. The tracking errors rapidly converge to nearly zero. Although the proposed tracker is designed under state quantization, its tracking performance is similar to that of the unquantized state feedback tracker [11] for MIMO pure-feedback nonlinear systems. Fig. 4 shows the control inputs u_1 and u_2 of the proposed approach. The estimates of W_i and δ_i, $i = 1, 2$ of the proposed approach are depicted in Fig. 5. These results demonstrate that satisfactory tracking performance is achieved by the proposed neural-network-based quantized state feedback tracker while ensuring that all the state variables and tracking errors are bounded.

Example 2: In this example, two inverted pendulums interconnected by a spring are taken as an example to verify the effectiveness of the proposed control strategy. The model is expressed as follows [45]:

$$\begin{aligned} J_1\ddot{\theta}_1 &= m_1 g L_p \sin(\theta_1) - 0.5 S_c L_p (L_d - S_\ell)\cos(\theta_1 - \theta_0) + u_1 \\ J_2\ddot{\theta}_2 &= m_2 g L_p \sin(\theta_2) - 0.5 S_c L_p (L_d - S_\ell)\cos(\theta_2 - \theta_0) + u_2 \end{aligned} \tag{66}$$

where θ_1 and θ_2 are pendulum angular positions, u_1 and u_2 are control torques, $m_1 = 1.5$ kg and $m_2 = 1.2$ kg are the masses, $L_p = 0.4$ m is the pendulum length, $J_1 = m_1 L_p^2$ and $J_2 = m_2 L_p^2$ are the moments of inertia, $D = 0.3$ m denotes the ground distance between two pendulums, $S_c = 45$ N/m and $S_\ell = 0.5$ m represent the spring constant and spring natural length, respectively, and L_d is the distance between the connection points, which is expressed as follows

$$L_d = \sqrt{D^2 + dL_p(\sin\theta_1 - \sin\theta_2) + \frac{L_p^2}{2}(1 - \cos(\theta_2 - \theta_1))}.$$

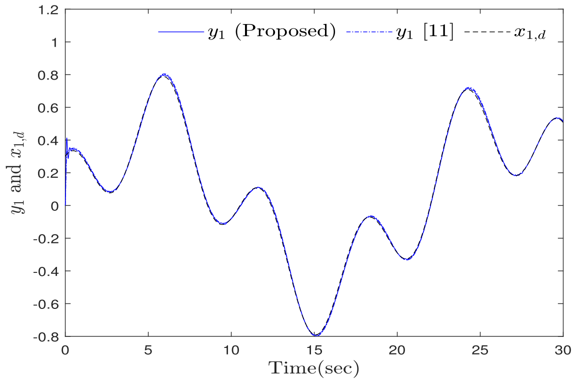

(a)

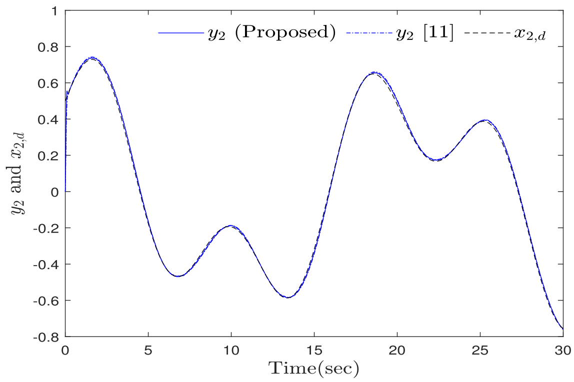

(b)

FIGURE 6. Tracking results for Example 2 (a) $x_{1,d}$ and y_1 (b) $x_{2,d}$ and y_2.

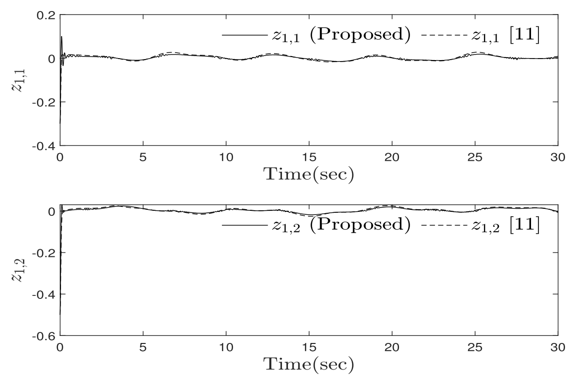

FIGURE 7. Control errors $z_{1,1}$ and $z_{1,2}$ for Example 2.

The relative angular position θ_0 can be defined as

$$\theta_0 = \tan^{-1}\left(\frac{0.5L_p(\cos\theta_2 - \cos\theta_1)}{D + 0.5L_p(\sin\theta_1 - \sin\theta_2)}\right).$$

Let us define the state variables $x_{1,j} = \theta_j$ and $x_{2,j} = \dot{\theta}_j$, and assume that the nonaffine nonlinear uncertainties $\Delta f_{1,j}$ and $\Delta f_{2,j}$ and the external disturbances $d_{1,j}$ and $d_{2,j}$, $j = 1, 2$, influence the system, as reported in [46]. The dynamics of (66) can then be rewritten as

$$\dot{x}_{1,1} = f_{1,1}(\boldsymbol{x}_1, x_{2,1}) + d_{1,1}$$

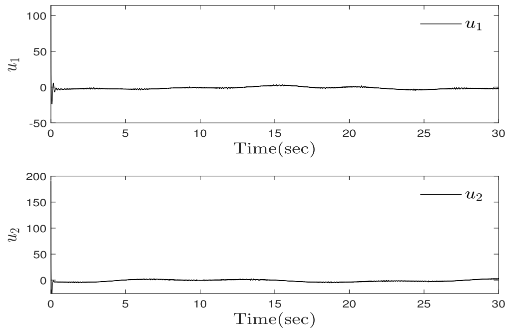

FIGURE 8. Control inputs u_1 and u_2 for Example 2.

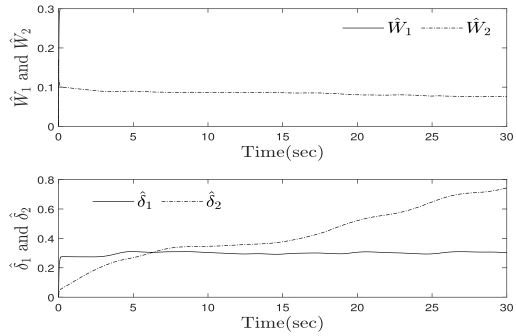

FIGURE 9. Estimates of W_1, W_2, δ_1 and δ_2 for Example 2.

$$\begin{aligned}\dot{x}_{1,2} &= f_{1,2}(\boldsymbol{x}_1, x_{2,2}) + d_{1,2}\\ \dot{x}_{2,1} &= f_{2,1}(\bar{\boldsymbol{x}}_2, u_1) + d_{2,1}\\ \dot{x}_{2,2} &= f_{2,2}(\bar{\boldsymbol{x}}_2, u_2) + d_{2,2}\end{aligned} \tag{67}$$

where $\boldsymbol{x}_1 = [x_{1,1}, x_{1,2}]^\top$, $\boldsymbol{x}_2 = [x_{2,1}, x_{2,2}]^\top$, $\bar{\boldsymbol{x}}_2 = [\boldsymbol{x}_1^\top, \boldsymbol{x}_2^\top]^\top$,

$$\begin{aligned}f_{1,1} &= x_{2,1} + \Delta f_{1,1}(\boldsymbol{x}_1, x_{2,1})\\ f_{1,2} &= x_{2,2} + \Delta f_{1,2}(\boldsymbol{x}_1, x_{2,2})\\ f_{2,1} &= J_1^{-1}[m_1 g L_p \sin(x_{1,1}) - 0.5 S_c L_p \cos(x_{1,1} - \theta_0)\\ &\quad \times (L_d - S_\ell) + u_1] + \Delta f_{2,1}(\bar{\boldsymbol{x}}_2, u_1)\\ f_{2,2} &= J_2^{-1}[m_2 g L_p \sin(x_{1,2}) - 0.5 S_c L_p \cos(x_{1,2} - \theta_0)\\ &\quad \times (L_d - S_\ell) + u_2] + \Delta f_{2,2}(\bar{\boldsymbol{x}}_2, u_2)\\ d_{1,1} &= 0.1\cos(2t), \quad d_{1,2} = 0.1\sin(2t)\\ d_{2,1} &= 0.2\sin(t), \quad d_{2,2} = 0.2\cos(t)\end{aligned}$$

with $\Delta f_{1,1} = 0.3\cos(x_{1,1}^2 x_{1,2})x_{2,1}$, $\Delta f_{1,2} = 0.2\sin(x_{1,1} \times x_{1,2})x_{2,2}$, $\Delta f_{2,1} = J_1^{-1}[(0.2 + 0.1\cos(x_{1,1}x_{1,2})) \times u_1]$, and $\Delta f_{2,2} = J_2^{-1}[(0.2+0.1\cos(x_{2,1}x_{2,2}))u_2]$. The desired signals are set to $\boldsymbol{x}_d = [0.5\sin(0.3t)+0.3\cos(\pi t/3), 0.3\sin(\pi t/4)+0.5\cos(0.3t)]^\top$. The initial conditions of the state variables are set to $\boldsymbol{x}_1 = [x_{1,1}, x_{1,2}]^\top = [0, 0]^\top$ and $\boldsymbol{x}_2 = [x_{2,1}, x_{2,2}]^\top = [0, 0]^\top$. The quantization level is set to $\rho = 0.01$. The design parameters are chosen as $\zeta_i = 18$, $\Gamma_{W,1} = 100$, $\Gamma_{W,2} = 10$, $\Gamma_{\delta,1} = 10$, $\Gamma_{\delta,2} = 0.2$, $\sigma_{W,i} = 0.1$, $\sigma_{\delta,1} = 0.5$, $\sigma_{\delta,1} = 1$, $\epsilon_{i,1} = \epsilon_{i,2} = 0.1$, $\bar{\varepsilon} = 0.25$, $\xi_{1,1} = \xi_{1,2} = 0.707$, $\varpi_{1,1} = 60$, and $\varpi_{1,2} = 80$ where $i = 1, 2$. The control gains and weight tuning parameters of the existing adaptive tracker [11] are set to be identical to those of the proposed tracker.

The tracking results and errors for *Example 2* are compared in Figs. 6 and 7. The tracking results of the position angles y_1 and y_2 are compared in Fig. 6. Fig. 7 shows a comparison of the tracking errors. Despite the quantization of state feedback signals, the proposed approach has a similar tracking performance to that of the previous adaptive tracker [11]. Fig. 8 illustrates the control inputs u_1 and u_2 of the proposed approach. The estimates of W_i and δ_i, $i = 1, 2$, of the proposed approach are displayed in Fig. 9. From these results, we conclude that the proposed adaptive neural tracker using quantized state feedback is effective in coping with unknown nonaffine nonlinearities of MIMO pure-feedback systems and state quantization.

V. CONCLUSION

We have presented a neural-network-based adaptive quantized state feedback control design and stability analysis strategies for uncertain MIMO block-triangular pure-feedback nonlinear systems with state quantization. The key aspect of the proposed strategy is that adaptive neural compensation terms using quantized states are derived to ensure the boundedness of the quantization errors of the closed-loop signals and to deal with unknown control coefficient functions derived from recursive designs. The adaptive neural tracker and its adaptive laws have been designed via quantized states, and the quantization errors have been compensated by the adaptive laws. By constructing technical lemmas for quantization errors and adaptive parameters, the uniform ultimate boundedness of all signals of the closed-loop system using quantized feedback is proved based on the Lyapunov stability analysis. Finally, the simulation results demonstrate that the proposed theoretical strategy provides effective control with good tracking performance. The neural-network-based quantized feedback tracking problem in the presence of measurement noise or faults will be investigated in future studies.

REFERENCES

[1] M. Krstic, I. Kanellakopoulos, and P. V. Kokotovic, *Nonlinear and Adaptive Control Design*. New York, NY, USA: Wiley, 1995.

[2] D. Swaroop, J. K. Hedrick, P. P. Yip, and J. C. Gerdes, "Dynamic surface control for a class of nonlinear systems," *IEEE Trans. Autom. Control*, vol. 45, no. 10, pp. 1893–1899, Oct. 2000.

[3] J. A. Farrell, M. Polycarpou, M. Sharma, and W. Dong, "Command filtered backstepping," *IEEE Trans. Autom. Control*, vol. 54, no. 6, pp. 1391–1395, Jun. 2009.

[4] Q. Shen and P. Shi, "Distributed command filtered backstepping consensus tracking control of nonlinear multiple-agent systems in strict-feedback form," *Automatica*, vol. 53, pp. 120–124, Mar. 2015.

[5] T. Zhang, S. S. Ge, and C. C. Hang, "Adaptive neural network control for strict-feedback nonlinear systems using backstepping design," *Automatica*, vol. 36, no. 12, pp. 1835–1846, 2000.

[6] S. S. Ge and C. Wang, "Adaptive NN control of uncertain nonlinear pure-feedback systems," *Automatica*, vol. 38, no. 4, pp. 671–682, Apr. 2002.

[7] Q. K. Shen, P. Shi, J. W. Zhu, S. Y. Wang, and Y. Shi, "Neural networks-based distributed adaptive control of nonlinear multiagent systems," *IEEE Trans. Neural Netw. Learn. Syst.*, vol. 31, no. 3, pp. 1010–1021, Mar. 2020.

[8] Q. Shen, P. Shi, R. K. Agarwal, and Y. Shi, "Adaptive neural network-based filter design for nonlinear systems with multiple constraints," *IEEE Trans. Neural Netw. Learn. Syst.*, vol. 32, no. 7, pp. 3256–3261, Jul. 2021.

[9] S. Tong and Y. Li, "Adaptive fuzzy output feedback control of MIMO nonlinear systems with unknown dead-zone inputs," *IEEE Trans. Fuzzy Syst.*, vol. 21, no. 1, pp. 134–146, Feb. 2013.

[10] Y. Cui, H. Zhang, Y. Wang, and H. Jiang, "A fuzzy adaptive tracking control for MIMO switched uncertain nonlinear systems in strict-feedback form," *IEEE Trans. Fuzzy Syst.*, vol. 27, no. 12, pp. 2443–2452, Dec. 2019.
[11] Z. Chen, S. S. Ge, Y. Zhang, and Y. Li, "Adaptive neural control of MIMO nonlinear systems with a block-triangular pure-feedback control structure," *IEEE Trans. Neural Netw. Learn. Syst.*, vol. 25, no. 11, pp. 2017–2029, Nov. 2014.
[12] Y. Zhou, W. Dong, Y. Chen, R. Zuo, Z. Liu, and S. Dong, "Robust adaptive control of MIMO pure-feedback nonlinear systems via improved dynamic surface control technique," *IEEE Access*, vol. 7, pp. 96672–96685, 2019.
[13] A. Boulkroune, L. Merazka, and H. Li, "Fuzzy adaptive state-feedback control scheme of uncertain nonlinear multivariable systems," *IEEE Trans. Fuzzy Syst.*, vol. 27, no. 9, pp. 1703–1713, Sep. 2019.
[14] M. Haddad, F. Zouari, A. Boulkroune, and S. Hamel, "Variable-structure backstepping controller for multivariable nonlinear systems with actuator nonlinearities based on adaptive fuzzy system," *Soft Comput.*, vol. 23, no. 23, pp. 12277–12293, Dec. 2019.
[15] H. Liu, T. Zhang, and X. Xia, "Adaptive neural dynamic surface control of MIMO pure-feedback nonlinear systems with output constraints," *Neurocomputing*, vol. 333, pp. 101–109, Mar. 2019.
[16] Y. Hua and T. Zhang, "Adaptive neural event-triggered control of MIMO pure-feedback systems with asymmetric output constraints and unmodeled dynamics," *IEEE Access*, vol. 8, pp. 37684–37696, 2020.
[17] G. N. Nair, "Quantized control and data-rate constraints," in *Encyclopedia of Systems and Control*. Berlin, Germany: Springer, 2015, pp. 1–9.
[18] R. W. Brocket and D. Liberzon, "Quantized feedback stabilization of linear systems," *IEEE Trans. Autom. Control*, vol. 45, no. 7, pp. 1279–1289, Jul. 2000.
[19] D. Liberzon, "Hybrid feedback stabilization of systems with quantized signals," *Automatica*, vol. 39, no. 9, pp. 1543–1554, Sep. 2003.
[20] S. W. Yun, Y. J. Choi, and P. G. Park, "H_2 control of continuous-time uncertain linear systems with input quantization and matched disturbances," *Automatica*, vol. 45, pp. 2435–2439, Oct. 2009.
[21] T. Hayakawa, H. Ishii, and K. Tsumura, "Adaptive quantized control for nonlinear uncertain systems," *Syst. Control Lett.*, vol. 58, no. 9, pp. 625–632, 2009.
[22] J. Zhou, C. Wen, and G. Yang, "Adaptive backstepping stabilization of nonlinear uncertain systems with quantized input signal," *IEEE Trans. Autom. Control*, vol. 59, no. 2, pp. 460–464, Feb. 2014.
[23] J. Zhou, C. Wen, and W. Wang, "Adaptive control of uncertain nonlinear systems with quantized input signal," *Automatica*, vol. 95, pp. 152–162, Sep. 2018.
[24] Y. H. Choi and S. J. Yoo, "Robust event-driven tracking control with preassigned performance for uncertain input-quantized nonlinear pure-feedback systems," *J. Franklin Inst.*, vol. 355, no. 8, pp. 3567–3582, May 2018.
[25] S. Song, J. H. Park, B. Zhang, and X. Song, "Composite adaptive fuzzy finite-time quantized control for full state-constrained nonlinear systems and its application," *IEEE Trans. Syst., Man, Cybern., Syst.*, vol. 52, no. 4, pp. 2479–2490, Apr. 2022, doi: 10.1109/TSMC.2021.3051352.
[26] W. Liu, Q. Ma, S. Xu, and Z. Zhang, "Adaptive finite-time event-triggered control for nonlinear systems with quantized input signals," *Int. J. Robust Nonlinear Control*, vol. 31, no. 10, pp. 4764–4781, 2021, doi: 10.1002/rnc.5510.
[27] K. Sun, H. R. Karimi, and J. Qiu, "Finite-time fuzzy adaptive quantized output feedback control of triangular structural systems," *Inf. Sci.*, vol. 557, pp. 153–169, May 2021.
[28] B. Niu, H. Li, T. Qin, and H. R. Karimi, "Adaptive NN dynamic surface controller design for nonlinear pure-feedback switched systems with time-delays and quantized input," *IEEE Trans. Syst., Man, Cybern., Syst.*, vol. 48, no. 10, pp. 1676–1688, May 2018.
[29] W. Liu, C. C. Lim, P. Shi, and S. Xu, "Observer-based tracking control for MIMO pure-feedback nonlinear systems with time-delay and input quantisation," *Int. J. Control*, vol. 90, no. 11, pp. 2433–2448, 2016.
[30] L. N. Bikas and G. A. Rovithakis, "Combining prescribed tracking performance and controller simplicity for a class of uncertain MIMO nonlinear systems with input quantization," *IEEE Trans. Autom. Control*, vol. 64, no. 3, pp. 1228–1235, Mar. 2019.
[31] K. Xie, Z. Lyu, Z. Liu, Y. Zhang, and C. L. P. Chen, "Adaptive neural quantized control for a class of MIMO switched nonlinear systems with asymmetric actuator dead-zone," *IEEE Trans. Neural Netw. Learn. Syst.*, vol. 31, no. 6, pp. 1927–1941, Jun. 2020.
[32] K. Zhao and J. Chen, "Adaptive neural quantized control of MIMO nonlinear systems under actuation faults and time-varying output constraints," *IEEE Trans. Neural Netw. Learn. Syst.*, vol. 31, no. 9, pp. 3471–3481, Sep. 2020.
[33] J. Zhou, C. Wen, W. Wang, and F. Yang, "Adaptive backstepping control of nonlinear uncertain systems with quantized states," *IEEE Trans. Autom. Control*, vol. 64, no. 11, pp. 4756–4763, Nov. 2019.
[34] Y. H. Choi and S. J. Yoo, "Quantized feedback adaptive command filtered backstepping control for a class of uncertain nonlinear strict-feedback systems," *Nonlinear Dyn.*, vol. 99, no. 4, pp. 2907–2918, Mar. 2020.
[35] Y. H. Choi and S. J. Yoo, "Neural-networks-based adaptive quantized feedback tracking of uncertain nonlinear strict-feedback systems with unknown time delays," *J. Franklin Inst.*, vol. 357, no. 15, pp. 10691–10715, Oct. 2020.
[36] Y. H. Choi and S. J. Yoo, "Distributed quantized feedback design strategy for adaptive consensus tracking of uncertain strict-feedback nonlinear multiagent systems with state quantizers," *IEEE Trans. Cybern.*, early access, Jan. 21, 2021, doi: 10.1109/TCYB.2021.3049488.
[37] W. Meng, Q. Yang, and Y. Sun, "Adaptive neural control of nonlinear MIMO systems with time-varying output constraints," *IEEE Trans. Neural Netw. Learn. Syst.*, vol. 26, no. 5, pp. 1074–1085, May 2015.
[38] M. M. Polycarpou, "Stable adaptive neural control scheme for nonlinear systems," *IEEE Trans. Autom. Control*, vol. 41, no. 3, pp. 447–451, Mar. 1996.
[39] G.-D. Hu and M. Liu, "The weighted logarithmic matrix norm and bounds of the matrix exponential," *Linear Algebra Appl.*, vol. 390, pp. 145–154, Oct. 2004.
[40] J. Park and I. W. Sandberg, "Universal approximation using radial-basis-function networks," *Neural Comput.*, vol. 3, no. 2, pp. 246–257, Mar. 1991.
[41] C. Wang, D. J. Hill, S. S. Ge, and G. R. Chen, "An ISS-modular approach for adaptive neural control of pure-feedback systems," *Automatica*, vol. 42, no. 5, pp. 625–635, 2006.
[42] A. J. Kurdila, F. J. Narcowich, and J. D. Ward, "Persistency of excitation in identification using radial basis function approximants," *SIAM J. Control Optim.*, vol. 33, no. 2, pp. 625–642, 1995.
[43] S. Sui, H. Xu, S. Tong, and C. L. P. Chen, "A novel prescribed performance fuzzy adaptive output feedback control for nonlinear MIMO systems in finite-time," *IEEE Trans. Fuzzy Syst.*, early access, Oct. 14, 2021, doi: 10.1109/TFUZZ.2021.3119750.
[44] S. Sui, C. L. P. Chen, S. Tong, and S. Feng, "Finite-time adaptive quantized control of stochastic nonlinear systems with input quantization: A broad learning system based identification method," *IEEE Trans. Ind. Electron.*, vol. 67, no. 10, pp. 8555–8565, Oct. 2020.
[45] W. KhanLin, Y. Lin, S. U. Khan, and N. Ullah, "Quantized adaptive decentralized control for interconnected nonlinear systems with actuator faults," *Appl. Math. Comput.*, vol. 320, pp. 175–189, Mar. 2018.
[46] R. Zuo, X. Dong, Y. Liu, Z. Liu, and W. Zhang, "Adaptive neural control for MIMO pure-feedback nonlinear systems with periodic disturbances," *IEEE Trans. Neural Netw. Learn. Syst.*, vol. 30, no. 6, pp. 1756–1767, Jun. 2019.

BYUNG MO KIM received the B.S. and M.S. degrees from the School of Electrical and Electronics Engineering, Chung-Ang University, Seoul, South Korea, in 2019 and 2021, respectively. His current research interests include non-linear adaptive control and intelligent control using neural networks.

SUNG JIN YOO (Member, IEEE) received the B.S., M.S., and Ph.D. degrees in electrical and electronic engineering from Yonsei University, Seoul, South Korea, in 2003, 2005, and 2009, respectively. He was a Postdoctoral Researcher with the Department of Mechanical Science and Engineering, University of Illinois at Urbana-Champaign, Champaign, IL, USA, from 2009 to 2010. Since 2011, he has been with the School of Electrical and Electronics Engineering, Chung-Ang University, Seoul, where he is currently a Professor. His research interests include non-linear adaptive control, decentralized control, distributed control, fault-tolerant control, and neural networks theories, and their applications to robotic, flight, non-linear time-delay systems, large-scale systems, and multi-agent systems.